Coordination Chemistry Reviews 252 (2008) 2552–2571

Contents lists available at ScienceDirect

Coordination Chemistry Reviews

journal homepage: www.elsevier.com/locate/ccr

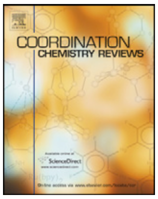

Review

Conformationally gated photoinduced processes within photosensitizer–acceptor dyads based on ruthenium(II) and osmium(II) polypyridyl complexes with an appended pyridinium group

Philippe P. Lainé[a,*], Sebastiano Campagna[b], Frédérique Loiseau[b,c]

[a] *Contribution from the Laboratoire de Chimie et Biochimie Pharmacologiques et Toxicologiques, UMR CNRS N° 8601, Université Paris Descartes, Faculté de Médecine, 45 rue des Saints Pères, F-75270, Paris Cedex 06, France*

[b] *Università di Messina, Dipartimento di Chimica Inorganica, Chimica Analitica e Chimica Fisica, Via Sperone 31, I-98166 Messina, Italy*

[c] *Département de Chimie Moléculaire, UMR CNRS 5250, Université Joseph Fourier, BP-53, 38041 Grenoble Cedex 09, France*

Contents

ARTICLE INFO

Article history:
Received 15 March 2008
Accepted 14 May 2008
Available online 21 May 2008

Dedicated to Dr. Jean-Pierre Sauvage.

ABSTRACT

This review deals with some identified consequences of excited-state conformational relaxations on photoinduced processes taking place within semi-rigid and potentially π-conjugated inorganic multicomponent systems. *Planarization* is the hallmark of structural upheavals herein considered. This ultrafast and widespread phenomenon is shown to occur upon various types of photoinduced charge redistributions at the intramolecular level, which span from mere metal-to-ligand charge transfer (MLCT) to charge separated (CS) state formation. Having first being reminded of the various aspects

---

Abbreviations: bpy, 2,2′-bipyridine; Me_2bpy, 4,4′-dimethyl-2,2′-bipyridine; tpy, 2,2′:6′,2″-terpyridine; ttpy, 4′-(*p*-tolyl)-2,2′:6′,2″-terpyridine; ptpy, 4′-phenyl-2,2′:6′,2″-terpyridine; phen, 1,10-phenanthroline; TP^+, 2,4,6-triarylpyridinium; TPH_3^+, 2,4,6-triphenylpyridinium; $TPH_2(NO_2)^+$, 2,6-diphenyl-4-*p*-nitrophenyl-pyridinium; $PyPh^+$, 4-phenyl-pyridinium.

* Corresponding author. Tel.: +33 1 42862086; fax: +33 1 42868387.
E-mail address: philippe.laine@univ-paris5.fr (P.P. Lainé).

doi:10.1016/j.ccr.2008.05.007

Keywords:
Metal polypyridine complexes
Supramolecular photochemistry/photophysics
Excited-state planarization
Conformational gating
Luminescence lifetime
Molecular switching

which constitute the general context of this review, that is supramolecular inorganic photochemistry, and put in perspective the plural status of intramolecular conformation, we shall assess the possible substantial changes in the photophysical features of luminophores following from planarization. Then, the impact of the excited-state planarization on the interplay between functional subunits via the modification of intercomponent electronic coupling, is discussed. Special emphasis is put on (closely coupled) dyads comprised of a photoactive coordination compound (typically of the ruthenium(II)-trisbipyridyl or osmium(II)-bisterpyridyl type) as both the photosensitizer and the primary light-triggered electron donor, and of a substituted pyridinium group as the electron acceptor. Implementation of conformational gating of photoinduced processes for molecular electronics or sensing devices is finally mentioned.

1. Introduction to light-triggered structural changes within coordination compounds

1.1. Background. Light absorption by coordination compounds of the d-block

Absorbing a photon is not a negligible event at the molecular level, in particular in the case of chromophoric coordination compounds based on transition metals of the *d*-block [1]. The hybrid nature of metallo-organic complexes is likely to reduce their chemical stability as compared, for instance, to chemical architectures relying on σ and π covalent bonds. The weakness of light-absorbing inorganic chromophores resides first in the nature of polar and dative metal–ligand coordination bonding. Secondly, photon absorption is correlated to excited-state intramolecular charge redistribution within the coordination sphere, which affects more or less directly the coordination bonds. This electronic reorganization can primarily involve either (i) *the metal* (M) *and the ligand(s)* (L) for instance on occasion of charge transfer (CT) transitions whether metal-to-ligand (MLCT) or ligand-to-metal (LMCT) and/or (ii) M–L *bonds* themselves on occasion of the population of metal-centered (MC) ligand-field (LF) states (d–d transitions), which have a destabilizing antibonding character and/or (iii) the *ligand only* in the case of purely ligand-centered (LC) transitions. Typically, given the same composition for the primary (first) coordination sphere of a metal cation, the splitting of d orbitals (Δ) originating from the ligand field increases with both the atomic number and the oxidation state of the metal center. For instance, in the case of a series of related complexes made up of a d^6 transition metal embedded within the pseudo-octahedral field of oligopyridyl ligands, the lowest-lying HOMO–LUMO electronic transition changes from a MC nature ($d(t_{2g}) \rightarrow d(e_g)$) for iron(II) to a MLCT nature ($d(t_{2g}) \rightarrow \pi^*(L)$) for both ruthenium(II) and osmium(II), to even purely LC transitions ($\pi(L) \rightarrow \pi^*(L)$) for rhodium(III) and iridium(III) ions [2–4]. As a consequence, divalent iron compounds are poorly stable upon light excitation (ligand-field – LF – photochemistry) while trivalent Rh and Ir complexes should be the most stable complexes of the series [5] as M–L bonds are not firstly affected by photoinduced charge redistribution (ligand-centered – LC – photochemistry). The same issues also hold for organometallic compounds [6].

1.1.1. Photoinduced structural changes within the chromophoric core (***P0***)

Structural relaxation processes (nuclear motion) take place [7] subsequent to light-energy absorption (vibronic transition) correlated with intramolecular redistribution of electron density to prepare the so-called Franck–Condon (F–C) initial state. The resulting sizable changes of the intramolecular geometry are also accompanied by a reorganization of surrounding medium such as solvent molecule repolarization. In general, electronic energy cascades downward very rapidly (femtosecond–picosecond timescale) from the F–C state, between various closely lying and vibrationally relaxed electronic levels within the excited-states manifold of the photoexcited compound. The lowest-lying electronic excited state (ES) is ultimately populated before the ground state (GS) is finally recovered. The return to the GS can occur via radiative and non-radiative transitions, whether by spin-allowed internal conversion (ic) or by spin-forbidden intersystem crossing (isc) processes. It is worth bearing in mind, however, that *luminescent* coordination compounds are only a minority. According to the rule put into words by Demas and Crosby [8] (analogous to the rule established by Kasha [9] for organic luminophores): in the absence of photochemistry from upper excited states, emission will occur from the lowest electronic excited state (general case) or from those states that can achieve a significant Boltzmann population relative to the lowest excited state. When the energy gap between the GS and lowest ES is too small, radiative deactivation pathway is no longer competitive with radiationless processes and the compound is non-luminescent. This is actually the reason why inorganic luminophores are *normally* not emissive in the IR domain and also the qualitative substance of the so-called “energy gap law” (the lower the emission energy the lower the emission quantum yield). The lowest-lying electronic excited state shows the longest lifetime and is the most completely thermalised that is, relaxed, including its environment. The lifetime of the lowest thermally equilibrated excited (thexi) state [10] is long enough to undergo large structural changes [7,11], contrary to other higher-lying excited states. All in all, the range of structural impacts subsequent to photoinduced electron density redistribution is very wide for chromophoric coordination compounds. It spans from:

(1) Mere disruption of M–L bonds (photolysis) with ligand ejection, as illustrated by the ligand release from photoexcited pentaammine(L)ruthenium(II) [12] and pentacyano(L)ferrate(II) complexes [13] resulting from LF and MLCT reactivities, respectively. Linkage isomerization of coordination bond(s) [14] is also possible, as in the case of the $Ru–O_{dmso}$ to $Ru–S_{dmso}$ photo-isomerisation within the $[(tpy)(bpy)Ru(dmso)]^{2+}$ complex [15,16];
(2) Dramatic distortions of the coordination sphere, as in the case of Jahn–Teller distortion of the tetrahedral ground state of $[Cu(phen)_2]^+$ towards a largely “flattened” MLCT excited state [17–21];
(3) “Breathing” of the inner coordination sphere essentially appearing as substantial changes in the M–L bond-lengths (possibly further complicated by changes of the spin state of M [22], as exemplified by the involved light-induced excited spin state trapping (LIESST) [23]);
(4) Barely impacted chromophores that is, almost no inner structural reorganization (as in the case of $[Ru(bpy)_3)]^{2+}$ [24]).

Noteworthy, large structural rearrangements are also efficient non-radiative pathways of deactivation; therefore, good inorganic luminophores are essentially rigid complexes of the latter class.

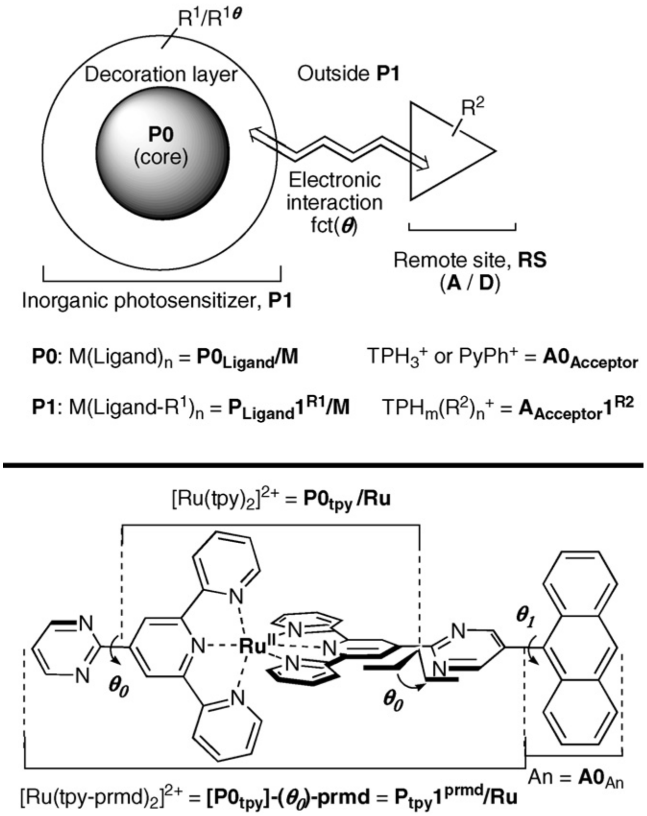

Fig. 1. (Top) Nomenclature adopted to describe two-component molecules formally comprised of a coordination complex as the photosensitizer (**P**; see text) connected by a single bond to a remote site (**RS**). Within the semi-rigid assemblies, the torsion angle (θ) is attached to intercomponent linkage. Equally, $R^{1\theta}$ are those substituents (R^1) of the chromophoric/luminophoric core (**P0**) showing a conformational (θ) degree of freedom (e.g. $R^{1\theta}$ = aryl). Here, **RS** can be an acceptor group (**A**). TPH_3^+, $TPH_m(R^2)_n^+$ and $PyPh^+$ refer to native 2,4,6-triphenyl-pyridinium (Figs. 7 and 8), R^2-substituted TP^+ ($R^2 = NO_2$; Fig. 8) and 4-phenyl-pyridinium (Fig. 7), respectively. (*Bottom*) Illustrative case of a compact semi-rigid assembly (cf. Section 1.4.4). The $[Ru(tpy)_2]^{2+}$ complex is the **P0** core, pyrimidinyl decorations (prmd) are $R^{1\theta}$ substituents belonging to **P1** (one the two prmd is also a rigid linker), and anthracene (An) is a remote site **RS** acting as a bare energy acceptor ($\mathbf{A_0}$).

The present review concentrates on robust metal complexes showing a low reorganizational level for the structure of their first (inner) coordination sphere (denoted as **P0** in Fig. 1) upon photon absorption, and moreover displaying at one and the same time good chromophoric and good luminophoric behaviors.

In the following, **P0** is the irreducible M/L assembly (with L naked that is, without any kind of substituents) corresponding to the core of the complex (reference parent) and the "second coordination layer" refers to decorations of **P0** to give **P1**. Here, the term "decoration" loosely refers to chemical groups grafted onto the **P0** core, regardless of their *functional role*: whether mere *substituents* or remote sites (**RS**) *full components* (Fig. 1).

1.1.2. Photoinduced structural changes around the chromophoric core (*P1*)

As a matter of fact, the actual electronic expanse of a chromophoric (and possibly luminophoric) species can extend beyond the "first" (inner) coordination sphere of the metal ion that is, the core **P0** (Fig. 1). Indeed, peripheral decorations ($R^1/R^{1\theta}$) of the primary ligands encompassed in **P1** (Fig. 1) are also involved. These extensions (R) can have a persistent electronic influence on the chromophoric features that is, on direct optical electronic transitions attached to photon absorption (case of electron-releasing and electron-withdrawing groups whether inductive or mesomeric; R^1 in Fig. 1). Also, they can have a delayed electronic influence, which is essentially revealed by the luminophoric features, when these decorations get involved in structural rearrangements subsequent to photoinduced charge redistributions (like those of MLCT character). Potentially π-extending groups are typically those molecular fragments involved in structure variations in the excited state such as conformational change about twist angle θ ($R^{1\theta}$ in Fig. 1). Hence, chromophores can have different electronic identities in the ground state and in the excited state, where they are actually operative as potential luminophores [10]. Getting a clear picture of the very nature of thexi states of chromophoric/luminophoric coordination compounds –including the impact of structural rearrangement of peripheral decorations – can facilitate their use as functional elements (typically: photosensitizers, **P**) within smart photoactive molecular assemblies. This knowledge is all the more desirable as π-extending substituents can also play the role of connectors between the components of these supramolecular arrays (e.g. between a photosensitizer, **P1**, and a remote site, **RS**; see Fig. 1).

We show here that conformational changes (θ) about the inorganic core of the photosensitizer on occasion of excited-state charge redistribution can play a determining role: from possibly impacting the luminophoric behavior of the **P** itself, up to gate photoinduced processes occurring within supermolecular assemblies in the excited-state.

1.2. Background. Using complex photosensitizers (*P*) within photochemical molecular devices (PMDs)

Balzani et al. introduced the paradigm of photochemical molecular devices (PMDs) two decades ago, with the aim of using light to trigger, monitor and fuel specific activities at the molecular level. The conceptual corpus perfected on purpose, supramolecular photochemistry [25–28], combines the backgrounds of inorganic photochemistry [29–33] and supramolecular chemistry [34]. Since the beginning, coordination compounds have played a central role as choice photosensitizers even if purely organic dye molecules may also be involved – as such – in the field [27,35]. On the one hand, photosensitizers (**P**) are used for interfacing intramolecular medium with the outside world, essentially operating in absorption for the input of light (tunable absorption energies and large absorption cross-sections are therefore desirable). Also, they often work in emission when light is viewed as an output, or simply because analysis of emitted light can be informative on the effectiveness of the photoinduced processes occurring at the intramolecular level [3]. On the other hand, **P** elements are also active functional components to initiate intramolecular electron (ET) and/or energy (EnT) transfers.

1.2.1. Transition metal complexes as photosensitizers (*P*)

In this context, transition metal complexes are appealing because of the unique richness of their electronic properties (chromophoric function for light absorption) as well as photophysical and photochemical behaviors, in particular with respect to photoredox activity. Basically, these features are closely related to the hybrid nature of complexes, including the often-dominating specific MLCT character and intervening spin–orbit coupling attached to the presence of metal cations with large atomic numbers (heavy-atom effect). Mixed organic–inorganic nature of complexes also facilitates interaction with light by allowing the fine-tuning of electronic properties according to a modular approach relying on the proper choice of both the metal ions and the ligands partners. M/L ingredients can be changed to customize absorption properties as well as to adjust the energy of the lowest-lying excited level (potentially reflected by the emission energy), which determines the efficiency of intramolecular photoinduced processes. But richness is often correlated with complexity. Once again, knowing excited-state structural changes about the primary coordination sphere (**P0** core) likely to impact the photophysical features of the lowest thexi state of an inorganic **P** element (e.g. **P1** in Fig. 1) and consequently its photochemical behavior within functional assemblies, is a prerequisite to successfully design PMDs and correctly interpret photophysical outcomes.

1.2.2. Inorganic PMDs for artificial photosynthesis

It is noteworthy that PMDs are in principle particularly well suited for performing artificial photosynthesis [36]. Functional modeling of the key photoinduced charge separation actually integrates the function of light harvesting (antenna system) and that of transducer for the conversion of light-energy into redox-energy, towards the preparation of charge separated (CS) or redox separated [30] states. Interestingly, charge transfer (CT) transitions within coordination compounds are the smallest photoinduced charge-separation processes one may think of, and that is regardless of the very nature of the resulting states: metal-to-ligand, ligand-to-metal or ligand-to-ligand (LLCT, including intra-ligand processes, ILCT). For instance, coordination compounds can behave as light-triggered reducing electron donors (via L^-) and oxidizing electron acceptors (via M^+) when photo-promoted in their MLCT states [3]. Moreover, electronic energy itself can also be donated by the photo-excited complexes that is, the neutral electron-hole pair of exciton quasiparticle can be transferred to energy acceptors. In other words, inorganic complexes are potentially suitable to photo-initiate intramolecular ET and EnT in addition to harvesting light for functional assemblies. Therefore, they can play the role of photosensitizers (**P**) within PMDs, especially for artificial photosynthesis.

Clearly, the spatial confinement of the excited state (for MLCT excited state, a sort of redox pair) within the photosensitizer **P** (whether **P0** or **P1**; Fig. 1) is connected to relatively short lifetime, while long "excited-state" (for excited state we here consider also charge separated states) lifetimes are needed to complete targeted light-to-chemical ultimate energy conversion. Hence, inspired by nature, increasing CS states lifetimes generally goes through the electrostatic decoupling of excitonic – Coulomb-correlated – electron-hole pairs, by further increasing their spatial separation. A widespread approach to this goal consists in gathering redox-active components (electron acceptors, **A** and donors, **D**) about the photosensitizer (the primary electron donor/acceptor) to attract the electron (located on L^-) and fill the associated hole (the vacancy located on M^+) by intramolecular ET. Using linkers (**lk**) to assemble various **P**, **A** and **D** elements is the way around hardly controllable diffusional (intermolecular) processes, and also a means to speed up the forward separation of the charges. Space and time monitoring of intramolecular processes is an underlying requirement to successfully achieve directional and sequential transfers whether of electrons or of electronic energy. Therefore, attached to the spatial layout of energy gradients (embodied by various electro-active subunits) within supramolecular architectures is the notion of *localized* descriptions. Then, the status of intercomponent electronic coupling supported by linkers becomes central [37]. Keeping a definite electronic identity (including redox potentials and key excited-states levels) for each functional component within the overall array is mandatory to make possible their synergistic work. Indeed, precepts of supramolecular – inorganic – photochemistry, as implemented to design photochemical molecular devices (PMDs) [25–27], rely on conveniently weak electronic coupling of functional subunits. Such functional assemblies are usually referred to as *supermolecules*.

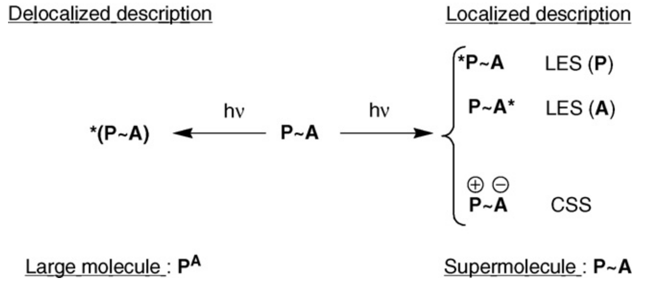

Fig. 2. Illustrative case of photosensitizer–acceptor bipartite molecules: $\mathbf{P}^{\mathbf{A}}$ "*large* molecule" behavior (*delocalized* description) versus **P**∼**A** "*supermolecule*" behavior (*localized* description) supporting locally excited states (LES) and/or charge separated state (CSS) formation from oxidative quenching (ET) of ***P** by **A**. The linker (∼) can either be a polyatomic molecular fragment or a single bond (θ).

1.2.3. Large chromophoric molecules versus photosensitized supermolecules (PMDs). The role of conformation within semi-rigid assemblies

In the representative "simple" case of a two-component molecule (Fig. 1), the status of the "remote site" (**RS**), *as such*, is attached to a *localized description* of the assembly (Fig. 2). The status of **RS** is indeed determined by both its intrinsic features with respect to those of **P** (actually ***P**) and the strength of the electronic coupling (interaction) mediated by the linker (**lk**). Hence, structural changes concerning the linker, such as conformational fluctuations, are likely to impact both the nature (electronic identity) of connected components and the development of intercomponent photoinduced processes.

RS can either be an acceptor **A** or a donor **D** of electron and/or of electronic energy with respect to photoexcited **P** (***P**), which also behaves as a dual (**D**/**A**) redox and electronic energy partner. Depending on the degree of intramolecular electronic coupling, one can distinguish between the following three kinds of assemblies.

- In the case of assemblies of type (A), **RS** is a genuine component for the reason that the intercomponent electronic coupling is conveniently weak and **RS** has no sizable direct electronic influence on **P**. **P** and **RS** essentially interact once **P** has been photoexcited (***P**) within the **P**–(**lk**)–**RS** array. The spacer (**lk**, symbolized by "∼" in the following) is typically made up of a saturated polymethylene chain or is comprised of a network of weak hydrogen bonding. In this context, if thermodynamically allowed, intramolecular intercomponent ET will occur according to a stepwise mechanism worth referred to as a photoinduced ET (PET) versus direct optical ET (that is, an electronic transition), which remains confined to the **P** component. For instance, for PET processes from the metal center of **P** to **RS** (**RS** = **A**), the electron is first promoted onto ligand(s) L (to form the primary MLCT state) before hopping to **RS**. This stepwise process can be assisted by surrounding solvent molecules as well as by orbitals of the linker. With respect to photoinduced electronic energy transfers (PEnT), the non-radiative coulombic mechanism (also referred to as the "through-space" or Förster mechanism [38]) is in principle [39] the only possible (if one excepts "trivial" radiative processes). It is based on the resonance of – large – transition moments attached to the concomitant deactivation of the energy donor (***P** → **P**) and activation of the acceptor (**RS** = **A** → ***A**). Alternative non-radiative short-range (double-electron)-exchange mechanism, also referred to as the "through-bond" or Dexter mechanism [40], requires orbital overlapping of **P** and **A** reactive partners that is, rather strong electronic coupling.

- In the case of assemblies of type (B), the electronic interaction between **RS** and **P** is substantial, so the electronic features and reactivity of both components are modified accordingly (as compared with parent isolated references), including in the ground state. Thus, **RS** behaves as both a *substituent* of **P** (and ***P**) and a *partner* of reactive ***P** for intercomponent processes. This intermediate situation is quite common when the linkers are partly unsaturated and/or short fragments (e.g. amide or aryl spacers). In this context, as far as thermodynamically allowed, stepwise photoinduced ET (attached to **P**∼**RS** behavior) can co-exist with direct optical ET to **RS** (attached to $\mathbf{P^{RS}}$ behavior, see below), as illustrated in Section 4. Similarly for intramolecular EnT processes: the two non-radiative mechanisms (Förster and Dexter) can be operative. Most importantly, PEnT (of Dexter type) and PET intramolecular processes can be in competition as they are both based on electron(s) transfer(s) (see Section 4).
- In the limit case of type (C), the intramolecular electronic coupling is so large that the whole assembly behaves as a novel made-in-one-piece electronic entity (*delocalized description*; Fig. 2), where **RS** is merely a substituent of **P** (denoted as $\mathbf{P^{RS}}$) or **P** a substituent of **RS** (denoted as $\mathbf{RS^{P}}$). In this case, notions of space and time monitoring as well as the related notion of *transfer* are no longer relevant, and the assembly is no longer a *supermolecule* (that is, a PMD) but rather a *large molecule* (e.g. a new *large* photosensitizer, $\mathbf{P^{RS}}$). This situation is typically encountered in compact assemblies when **P** and **RS** are directly linked that is, when there is virtually no linker but a single bond only.

In the borderline case of compact assemblies and as far as the local molecular structure about the intercomponent linkage is semi-rigid, the electronic interplay between functional subunits can be modulated, in principle continuously, by a single torsion angle (θ), functioning “as the linker” (“∼” = (θ)). This particular situation may give a unique opportunity to address the question of the upper limit of intramolecular electronic coupling (possibly related to a critical value of θ) above which “supermolecular” behavior (denoted as **P**-($\boldsymbol{\theta}$)-**RS**) is switched to “large molecule” behavior (denoted as $\mathbf{P}(\boldsymbol{\theta})^{\mathbf{RS}}$) that is, when the relevance of a localized description (Fig. 2) of photoinduced events actually vanishes for a given intramolecular context. This point is of importance since (1) conformational changes can occur in the excited state upon charge redistribution and (2), achieving long-lived CS state formation (normally proper to supermolecules) within closely coupled assemblies has recently emerged as a challenge in the field of artificial photosynthesis [41–45]. The very nature of photoinduced phenomena taking place within electronically closely coupled and spatially compact molecules is also of basic interest, including for the related field of molecular electronics and also for the switching effect at the molecular scale.

1.3. Background. Focusing on planarization versus twisting as preferential photoinduced structural relaxation of photosensitized semi-rigid assemblies

From a general viewpoint, besides usual structure fluctuations (including torsional motions) attached to surrounding thermal bath, one can identify two types of structural changes within semi-rigid molecules, which are classified as a function of the nature of their *ultimate* trigger. (1) The ultimate trigger is *internal,* as is typically the case for structure *relaxation* subsequent to intramolecular electron density redistribution, regardless of the nature of the primary – external – trigger for the charge redistribution itself (whether light or other); (2) the ultimate trigger is *external,* as is the case for structure change upon applying a mechanical constraint at the molecular level whether resulting from a chemical perturbation (e.g. complexation reaction) or other [46,47]. Here, we are essentially interested in conformational changes of the first type (1), which is related to photoinduced changes in intramolecular charge distribution.

In the field of organic photophysics and photochemistry, there are many reports on molecules showing a substantial *structure relaxation* subsequent to – photoinduced – charge redistribution at the intramolecular level. Arguably the most studied is the textbook case of the so-called twisted intramolecular CT (TICT effect), occurring within compact donor–acceptor molecules upon light excitation [48]. In the benchmark example of DMABN, the **D** (*N*,*N*-dimethylamino) and **A** (benzonitrile) subsystems are linked by a single bond and molecular geometry adapt to the change of the intramolecular distribution of electron density by adopting a perpendicular conformation (twist between the planes of $\mathbf{D^+}$ and $\mathbf{A^-}$, $\theta \approx 90^\circ$) in the lowest thexi state (in polar solvents) while the molecule is roughly coplanar ($\theta \approx 0^\circ$) in the neutral GS [48].

On the other hand, it is well established that the canted rings of oligophenylene-like molecules in their (neutral) native form become coplanar when these semi-rigid assemblies are reduced [49,50], oxidized [51,52] or photoexcited [53], as a result of an emerging quinoïd pattern. In other words, the *planarization* of the architecture is, in this case, the preferential mode of structure relaxation.

Hence, the question arises whether *planarization* or *twisting* is the kind of conformational *relaxation* one may expect within herein examined inorganic assemblies, in addition to thermally activated fluctuating contributions to conformational motions.

In the case of the MLCT excited-state reactivity of interest here, the electron donor is primarily the metal cation (M) embedded within the **P0** core of the photosensitizer and the primary electron acceptors are the ligands (L) also forming **P0**. Hence, the only possible structural adaptation to electron density redistribution within these made-in-one-piece robust chromophoric coordination compounds is via slight variations of M–L bond-lengths and bite angles (see Section 1.1.1), conversely to TICT species. Dominating reactivity is that of reduced organic part of the inorganic assembly comprised of primary ligand(s) and decoration(s) or extension(s). Indeed, MLCT electronic transitions (and possibly ensued CS processes) are widely recognized as light-triggered intramolecular redox reactions where the metal center is oxidized while ligands (and possibly their extensions) are reduced [11,54]. Therefore, *planarization* [55] (versus *twisting*) is anticipated to be the preferential pathway for structure relaxation of semi-rigid inorganic assemblies (whether **P-(**$\boldsymbol{\theta}$**)-RS** supermolecules or $\mathbf{P}(\boldsymbol{\theta})^{\mathbf{RS}}$ large molecules) in their lowest thexi state.

Actually, whether *twisting* (increasing θ) or *planarization* (decreasing θ), the very nature of light-triggered torsional motions is closely dependent on the topological features of active molecular orbitals (MOs). The MOs to be filled or emptied are indeed characterized by bonding or antibonding contributions about key interannular linkages. For instance, the quinoïd pattern of the LUMO of oligophenylene molecule largely accounts for the structural planarization upon reduction. More precisely, structure relaxation subsequent to charge redistribution is the average result of weighted contributions originating from various MOs populated and depopulated on occasion of net charge redistribution [56].

1.4. Background. Ru(II) and Os(II) polypyridyl complexes as the photosensitizers of compact semi-rigid architectures

To properly assess the aforementioned basic issues, both the **P** functional element and its surrounding intramolecular medium must be determined.

1.4.1. *Features of the lowest thexi state of the photosensitizers*

On the one hand, luminescence is basically not required *as such* for the photosensitizer **P** to successfully achieve its dual function (light absorption and primary electron donor/acceptor) [57] that is, for PMDs specifically designed for photoinduced charge separation. Therefore, any MLCT state is in principle suitable to initiate intramolecular ET, regardless of its spin multiplicity. It remains nonetheless that, to allow intramolecular photochemistry to fully develop from MLCT states, long-lived excited-state(s) are preferred to the short-lived ones, hence the pivotal role of the lowest thexi state (see also Section 1.1.1). The spin-forbidden nature of the electronic transition from the MLCT excited state to the ground state is therefore highly desirable to prolong the lifetime of the lowest thexi state.

On the other hand, luminescence is a required property for other types of PMDs designed for the related field of sensing devices and molecular electronics/photonics, in particular for advanced prototypes intending to process photons as inputs and/or outputs. For instance, to get around detrimental environmental background of natural luminescence, increased emission lifetime of the **P** component of sensor PMDs is usually preferred to enhanced emission intensity. Thus, once again, phosphorescence is preferred to fluorescence.

In these contexts, insights gained into the processes likely to govern light emission of ***P** such as intramolecular oxidative quenching attached to the aforementioned photochemistry, may be turned to account for the rational design of smart molecular devices.

Brought together, these issues indicate that the suitable lowest thexi state of **P** for PMDs intended for either artificial photosynthesis or molecular sensing applications should have a spin multiplicity different from that of the ground state, and giving rise to phosphorescence when emissive. Typically, in the case of closed-shell transition metal complexes showing a diamagnetic ground state (singlet state), as is the case of d^6 metals embedded within a strong ligand field of (pseudo)octahedral symmetry, the lowest thexi state is a triplet MLCT (^{3}MLCT).

1.4.2. *Absorbing light in the visible-NIR range (artificial photosynthesis purposes)*

Under favorable conditions (roughly speaking: a sunny day at noon and at sea level), typical solar spectral irradiance ($W\,m^{-2}\,nm^{-1}$) on the Earth is distributed as follows: near-UV: 5% (UV radiation is largely filtered by the atmosphere [58]), visible ($400\,nm \leq \lambda \leq 700\,nm$): 43% and IR: 52% [59]. On the other hand, far-infrared radiation is not useful, as it cannot induce electronic transitions (see also Section 1.1.1). Therefore, quantum conversion of solar energy relying on at least a primary photochemical process requires photosensitizers absorbing light essentially in the visible and near-IR domains. It is also noteworthy that this range of energy is indeed compatible with the achievement of chemical reactions of interest for energy storage [58,59] so that sunlight is worth harvesting. In this context, arguably the most fascinating process is the splitting of water molecules into molecular dihydrogen and dioxygen ($H_2O = H_2 + 1/2O_2$) [60]. Water does not absorb solar radiation hence oxidation–reduction reactions involved in the splitting process need to be photosensitized. The free energy of this benchmark process is 1.23 eV, corresponding to a photon at a wavelength of 1008 nm. Actually, this value *formally* translates as the minimum energy gap between the lowest thexi state (responsible for the photochemistry) and the ground state (that is, the threshold energy for water splitting [61–63]), provided that excited-state redox potentials of the photosensitizer lie properly with respect to water oxidation and proton reduction [30,62,64].

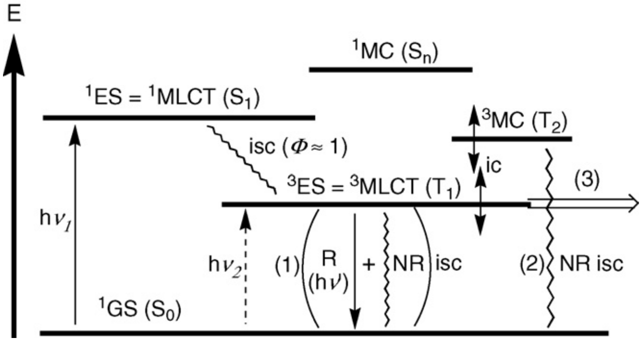

Fig. 3. Simplified scheme based on the relevant levels and processes accounting for both electronic absorption ($h\nu_1$, $h\nu_2$) of **P** and photophysical (1 and 2) versus photochemical (3) behavior arising from the pivotal ^{3}ES (^{3}MLCT lowest thexi state) of ***P**: (1) isc radiative (R) decay (phosphorescence, $h\nu'$) plus non-radiative (NR) isc deactivation (wavy line) and (3) photochemistry including PET and PEnT processes; (↔): interplay of the ^{3}MLCT with the ^{3}MC level via thermally activated internal conversion (ic) and subsequent radiationless isc (2) to the GS. Effects of intervening excited-state relaxations are omitted for clarity.

The present paper therefore concentrates on molecular photosensitizers, which are chromophoric coordination compounds absorbing light essentially in the visible and near-IR domains [65] in addition to emitting light (phosphorescence) as one of the preferential means to recover their ground state (luminophore behavior).

1.4.3. *Selecting Ru(II) and Os(II) polypyridyl complexes as the photosensitizers*

Over the years, in the field of inorganic photophysics and photochemistry, polypyridyl complexes of d^6 transition metals, in particular tris(diimine) and bis(triimine) compounds, have emerged as the most appealing and popular photosensitizers [29,54,66]. Among them, there are Rh(III) [67] and Ir(III) [68] polypyridyl complexes; unfortunately, these are barely colored (essentially UV-absorbing chromophores; Section 1.1) and their photochemistry is dominated by LC transitions. Hence, they do not fulfill the afore-identified requirements. With respect to Re(I) complexes, they are often mixed polyimine-carbonyl derivatives classified among *organometallic* rather than *coordination* compounds. Even if their electronic, photophysical and photochemical behavior is rich and to various extent based on an MLCT reactivity [69], they will not be further discussed here, as they usually absorb light essentially in the near-UV/near-visible domain ($\lambda < 450\,nm$). Finally, Ru(II) [70] and Os(II) [71] polypyridyl complexes are more suitable because of the proper balance they show between (1) large absorption cross-section ($\varepsilon \geq 10^4\,M^{-1}\,cm^{-1}$) in the visible range [72] (with possible extension towards NIR for Os-based species, thanks to partly allowed ^{3}MLCT transitions [73] as a result of large spin–orbit coupling) and (2) stability towards light irradiation. Of importance, also, intersystem crossing (isc) between the lowest ^{1}MLCT state (S_1) and the ^{3}MLCT lowest thexi state (T_1) is very rapid (femtosecond timescale) [11] and highly efficient ($\Phi_{isc} \approx 1$) [74]. This quantitative conversion of S_1 into T_1 gives to the lowest thexi state of these polyimine complexes its pivotal role even though this role also depends on an upper-lying state of the same spin multiplicity (triplet) but of different nature (MC), namely the thermally accessible ligand-field (dd) state $^3[(d\pi)^5(d\sigma^*)^1]$.

1.4.4. *On the complexity of tuning excited-state properties of Ru(II) and Os(II) polypyridyl complexes*

Photoinduced processes attached to Ru(II) and Os(II) polyimine photosensitizers are summarized in Fig. 3. Noteworthy, photochemistry (pathway 3) usually occurs to the detriment of emission (pathway 1). Similarly, populating the ^{3}MC state, which undergoes highly efficient radiationless deactivation to the GS (pathway 2) [54], bypasses pathway (1). Hence, analysis of the luminescence of **P**-containing molecular assemblies is a valuable means to obtain information on the effectiveness of intramolecular photoinduced processes. To what extent these processes (paths 1, 2 and 3) can be tuned (gated) by conformational parameters is the question addressed in the present review, which is essentially assessed on the bases of photophysical issues.

P is potentially an electron donor/acceptor (for charge separation) and an electronic energy donor (for electronic energy transfer) by virtue of its lowest-lying ^{3}MLCT state (T_1). There are three main strategies which may be used to tune the photophysical and photochemical features of **P**. On the one hand, adjusting the ^{3}MLCT–^{3}MC energy gap (parameter *a*) and modifying intrinsic features of the ^{3}MLCT level by playing on the extent of intraligand electronic delocalization (parameter *b*) are the usual means to control the lifetime of the lowest thexi state. On the other hand, adjusting the energy of T_1 normally goes through changing the ^{3}MLCT–GS energy gap (parameter *c*). The point is that all three parameters (*a*, *b* and *c*) are more or less interrelated so they cannot be varied independently. Changing any of the first two parameters (*a* and *b*) also impacts the ^{3}MLCT–GS energy gap (parameter *c*) and vice versa. There exists however a fourth and recently perfected approach (parameter *d*) [75] worthwhile to be outlined. This is distinguishable from the first three in that pathway (1) is regulated by reversible energy transfer (equilibration) via pathway (3) [76] without perturbing any of the key energy gaps (parameters *a* and *c*) of **P** (*supermolecular* behavior of type (A) in Section 1.2.3) [77]. This sophisticated strategy aiming at increasing the lifetime of T_1 [78] relies on the use of a remote site appended to **P** (**RS** in Fig. 1) as a temporary energy reservoir [77,79] (cf. Section 1.4.4.2 below).

Fortunately, the complexity and subtlety devoted to the task of tuning the excited-state features of **P** is somewhat alleviated by the synthetic versatility of Ru(II) and Os(II) polypyridyl complexes, which actually largely stems from their kinetic inertness as compared with similar, but labile, iron(II) compounds, subject to ligand redistribution in solution [80]. This valued chemical stability allows one designing bis- and even tris-heteroleptic compounds [81]. Various approaches aiming at manipulating the properties of MLCT excited states (and especially the lifetime of T_1) are well documented [77,82–89]. They can be categorized into *coarse-tuning* those modifications concerning the core of **P** (that is, **P0**; Fig. 1), and *fine-tuning*, those adjustments concerning the decoration layer of **P0** (encompassed in **P1**) as well as the **RS** when present (case of approach based on parameter *d*).

1.4.4.1. Coarse- and fine-tuning of excited-state properties of Ru(II) and Os(II) polypyridyl complexes. Whether working in the absorption or emission regime (attached to excited-state behavior), basically the same types of states (MLCT and MC) are involved. Therefore, it is not surprising that the tuning of electronic features of **P** as a chromophore [89,90] or a luminophore [83,84] relies on virtually the same principles. For instance, increasing the ligand field increases the energy gap between the $^1[(t_{2g})^6(e_g)^0]$ singlet state (corresponding to the GS, S_0) and the $^{(2S+1)}[(t_{2g})^5(e_g)^1]$ excited “dd” states (also denoted as $^{(2S+1)}[(d\pi)^5(d\sigma^*)^1]$, whether $^1[(t_{2g})^5(e_g)^1]$ or $^3[(t_{2g})^5(e_g)^1]$ referred to as ^{1}MC (S_n) and ^{3}MC (T_2) levels, respectively; Fig. 3). Similarly, lowering the energy of the LUMO (here a π^* orbital of the electron-accepting ligand) decreases the energy of the corresponding MLCT states (whether ^{1}MLCT or ^{3}MLCT), revealed by a bathochromic shift of the absorption band (^{1}MLCT state formation) and a red-shifted emission band (originating from the ^{3}MLCT state). In the following, we essentially focus on the tuning of excited states features as photoinduced processes are of main interest here.

The *coarse-tuning* is primarily concerned with the strength of the ligand field (represented by the d orbitals splitting, $\Delta = 10Dq$) and is obviously directly related to the composition of **P0** (including M and L). Photoinduced ligand dissociation speaks for the prominent contribution of the ligand field. Although usually neglected, however, Ru(II)-polypyridyl complexes suffer slight photodecomposition when potentially coordinating counter-anions are present in solution [91–94]. This detrimental ligand dissociation [95] is ascribed to thermal population of the upper lying T_2 level (MC) from T_1 [54]; this is the reason why osmium-based analogues, featuring a *ca.* 30% larger ligand field, are virtually not concerned by photolabilization [2]. Actually, given a formal common composition for the $\mathbf{P0_L}$/**M** core (see nomenclature in Fig. 1), for instance a ruthenium(II) complex comprised of six pyridine rings (whether py, bpy, tpy, higher oligo-py, other py-based ligands), Δ is closely related to the inner symmetry of the coordination sphere and the presence of strains about the metal center related to four-/five-membered chelate rings (resulting in M–L bond elongation and bite angle deformations). Thus, Δ decreases on deviating from ideal *Oh* symmetry: being larger for the D_{3h} $[Ru(bpy)_3]^{2+}$ species (denoted $\mathbf{P0_{bpy}}$/**Ru**) than for the trans-meridional D_{2d} $[Ru(tpy)_2]^{2+}$ complex (denoted $\mathbf{P0_{tpy}}$/**Ru**). Basically, this change of Δ and consequently the thermal accessibility of the ^{3}MC state explains the poor room-temperature photophysical properties of the bis-terpyridyl complex (almost non-luminescent) as compared with the tris-bipyridyl one (nicely phosphorescent) [54]. On this basis, introducing strains in the close vicinity of the transition metal (including playing on inter-ligand steric hindrance) allows one to make the ligand field conveniently weak on-purpose to switch the magnetic properties of the polyimine complexes from the usual diamagnetic low-spin state ($S = 0$) to the rare high-spin state ($S = 2$) [96] or to favor photoinduced ligand ejection, turned to good account to build light-driven molecular machines or muscles [97]. Conversely, optimizing the coordinating pattern of polydentate ligands so as to minimize inner-**P0** strains (e.g. by arranging six-membered chelate rings and hence increase Δ) is a means to dramatically improve the photophysical features of luminophores with respect to the lifetime of the lowest thexi state (T_1). This strategy has been successfully applied to obtain photosensitizers combining the appealing structural features of rod-like [98] pseudo trans-meridional bis-triimine complexes $[Ru(L_2)]^{2+}$ (L = 2,6-bis(8′-quinolinyl)-pyridine: a tpy-like ligand) with great photophysical properties similar to those of reference tris-diimine complexes represented by archetypal $[Ru(bpy)_3]^{2+}$ [99]. Last, it is worth noting that, besides gaining in chemical stability and also possibly in π-delocalization (see below) [87,100], the rigidity provided by the use of oligo-[*n*]dentate ligands (instead of *n* monodentate ligands) also greatly contributes to the photophysical improvement of **P0** by reducing the weight of non-radiative decay from T_1 (Fig. 3), including by cage-like effects [101].

Once the basic **P0**/**M** motif has been selected, *fine-tuning* comes into play to customize electronic properties of **P** in the form of the **P1**/**M** derived family (Fig. 1). Roughly, for the R^1 type of decorations (Fig. 1) whether of purely inductive character (±*I*) or of mixed inductive (±*I*) – mesomeric (±*M*) nature, electron-donating substituents (+*I*/*M*) are more destabilizing for the MC ground state that is, the filled metal $(d\pi)^6$ orbital (HOMO), than for the lowest-lying empty π^* orbital of L (LUMO). On the other hand, electron-withdrawing substituents (−*I*/*M*) are more stabilizing for the π^* orbital of L than for the MC ground state [84]. In other words, both types of substituents contribute to decrease the ^{1}MLCT–GS energy gap, thus leading to a bathochromic shift of the MLCT absorption band(s) as compared with reference parent **P0**. As a consequence, emission is red-shifted accordingly. Moreover, heteroleptic compounds related to the same **P0** core and carrying both electron-accepting and electron-donating R^1 substituents always absorb and emit photons at lower energy than parent reference homoleptic complexes (**P0**) due to cumulated electronic effects of the two types of decorations (namely lowered energy of the LC π^* orbital (LUMO) by the acceptor and energy-destabilized $d(\pi)$ MC HOMO by the donor) [84]. There exists however a basic difference between electron-donating and electron-withdrawing R^1 substituents when referring to the strength of the ligand field. On the one hand, taking the bare **P0** parent as the reference, electron-accepting substituents further diminish inter-electronic repulsion within the filled $d(\pi)$ orbitals (greater nephelauxetic effect), thus stabilizing this component and increasing the ligand field splitting of the d orbitals (Δ) [102], and thereby enlarging the ^{3}MLCT–^{3}MC gap (parameter *a*). On the contrary, electron-donating substituents contribute to increase inter-electronic repulsion within filled $d(\pi)$ orbitals of the HOMO (weakened nephelauxetic effect as compared with that effective within native **P0**), which is energy-destabilized accordingly, hence the correlated reductions of both Δ and the ^{3}MLCT–^{3}MC gap (parameter *a*). Therefore, depending on the balance between detrimental effects of energy gap law (reduced ^{3}MLCT–GS gap (parameter *c*)) and beneficial contribution of reduced thermal accessibility of dd states (^{3}MC) from T_1 (enlarged ^{3}MLCT–^{3}MC gap (parameter *a*)), electron-accepting R^1 decorations do not systematically result in the shortening of the key lifetime of T_1, conversely to electron-donating groups. Generally, depending on whether the weight of the radiationless decay via the dd pathway is low or high for a given **P0** core that is, whether **P0** is basically a good (e.g. $\mathbf{P0_{bpy}}$) or a poor (e.g. $\mathbf{P0_{tpy}}$) luminophore, the red-shifted emission of the derived **P1** series of photosensitizers obtained by the decoration of **P0** will be respectively more [30,88,89,103] or less [84] sensitive to energy gap law.

Regarding the extension of the lifetime of the T_1 MLCT excited-state, one of the most efficient fine-tuning method consists of arranging increased electron delocalization over the acceptor ligand by extending its conjugated π-bonding framework (aforementioned strategy based on parameter *b*) [87,100,104]. Basically, this approach is aimed at averaging structural distortions (ΔQ_e) attached to the presence of photo-promoted electron on the ligand and by increasing the number of π-bonds mobilized to support this electron. The difference in the equilibrium displacement (ΔQ_e) between the lowest thexi state (T_1) and the ground state (S_0), is therefore minimized and so is the magnitude of the vibrational overlap between T_1 and S_0. Related to this latter integral (Franck–Condon factor), the rate constant for non-radiative decay (k_{nr}) of T_1 is decreased accordingly and the lifetime of T_1 is thus increased.

Together with increased rigidity of the ligand framework (often attached to the design of "large-surface ligand"), which also results in a decrease of k_{nr} following the minimized change in the ΔQ_e between T_1 and S_0 [87,100,104], the "delocalization strategy" (parameter *b*) has been successfully applied to circumvent the detrimental effects of the energy gap law for NIR emitters [83,105,106]. Moreover, when appropriately combining their electron-donating and withdrawing decorations [83,89], ruthenium and osmium complexes of these polypyridyl-based (or derived) large-surface ligands are often choice candidates as panchromatic dyes (colloquially known as black absorbers [107]).

Another illustrative implementation of the "delocalization strategy" concerns the lifetime improvement of the lowest thexi state of trans-meridional bis-triimine complexes of ruthenium(II) (represented by $[Ru(tpy)_2]^{2+}$, denoted $\mathbf{P0_{tpy}}$/**Ru**), which are of pivotal interest to build linear PMD arrays meant to photo-produce long-lived charge-separated states [80,86]. This important issue has been subject, also, to a great deal of effort at the coarse-tuning level [99] (cf. Section 1.4.4.1). Thus, instead of appending the usual phenyl substituent at the 4′-position of tpy to expand the π-framework of the tridentate ligand (see Section 2), Hanan and co-workers have proposed to exploit the sterically less demanding 2-pyrimidinyl (prmd) ring [108,109]. In doing so, two fine-tuning parameters are actually changed:

(i) The π-extending conjugation is reinforced insofar as there is a steric decongestion about the interannular linkage, between the central ring of the tpy (part of the $\mathbf{P0_{tpy}}$ core) and the dangling pyrimidinyl ring. The tpy and prmd moieties (with attached dihedral angle θ_0) are then allowed to lie in an almost coplanar fashion in the ground state, as demonstrated by X-ray diffraction: $\theta_0 < 10^\circ$ [108,110] versus *ca.* 25° on the average for phenyl-substituted tpy analogues [111].

(ii) The π-accepting (electron-withdrawing) character of the substituent is reinforced as compared with phenyl group due to the heterocyclic nitrogen atoms of the pyrimidinyl fragment. As previously explained, this latter factor contributes to enlarge the ^{3}MLCT–^{3}MC energy gap and therefore to reduce the efficiency of the radiationless deactivation pathway (2) (Fig. 3) via thermal population of the ^{3}MC level.

Acting together, these effects result in a significant improvement of the photophysical features of the $\mathbf{P0_{tpy}}$/**Ru** luminophore when embedded within the $[(tpy)Ru(tpy\text{-}prmd)]^{2+}$ complex (denoted $\mathbf{P0_{tpy}(\boldsymbol{\theta_0})^{prmd}}$/**Ru** with prmd as a $R^{1\theta}$ substituent of the core $\mathbf{P0_{tpy}}$, also labeled as $\mathbf{P_{tpy}1^{prmd}}$/**Ru**; cf. Fig. 1). Typically, the emission lifetime is multiplied by a factor of 30, increasing from 0.25 to 8 ns.

1.4.4.2. When conformational modulation of excited-state properties of Ru(II) and Os(II) polypyridyl complexes comes into play. Particular attention deserves to be paid to those substituents having a *mesomeric* electron-accepting character (usually denoted as *-M*) such as *conjugated* aryl groups showing a conformational degree of freedom (θ) ($R^{1\theta}$ in Fig. 1), in contrast to other π-extending R^1 substituents like nitrile or ethynyl fragments, which display symmetry of revolution. Indeed, besides lowering the energy of the LUMO (LC π^* orbital) and allowing extended electron delocalization, they can be involved in structural relaxations subsequent to the intramolecular charge redistribution attached to the formation of MLCT states: namely a *planarization* upon ligand reduction (Section 1.3). The point is that the change of the twist angle θ – moreover towards (co-)planarity, – which amounts to promoting intraligand conjugation, is precisely likely to impact (favorably) the lifetime of T_1 (cf. Section 1.4.4.1).

Intramolecular conformation also plays a role when the tuning of the photophysical properties of **P** relies on the use of one or more appended remote(s) site(s) (**RS**). As a matter of fact, there is a multiplicity of potentially operative pathways at the intramolecular level when dealing with PET and PEnT processes. Following the realization that, for PMDs, ill-defined structures may impact negatively on their functional working mode –suffice to mention the detrimental effects of intramolecular short-circuits within flexible assemblies – [112–114], fine-control of the overall geometry of multicomponent assemblies has emerged as a key issue, and there is now a general propensity to design (semi)-rigid architectures [111,114–117]. This is, for instance, the case for the multichromophore approach aimed at increasing the lifetime of the lowest thexi state of inorganic **P** (cf. strategy based on parameter *d*; Section 1.4.4) [77]. The **RS** used are organic chromophores capable of accepting electronic energy (**RS** = **A**) and temporarily store it, thus acting as reservoir(s) to delay MLCT decay and thereby increasing its lifetime. Providing the subtle balance between proper kinetic and thermodynamic parameters attached to **P** and **RS** (**A**), the concept is based on equilibration processes namely reversible intercomponent **P** ←(path

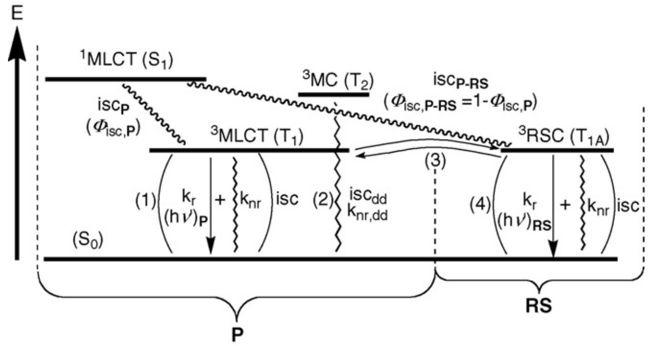

Fig. 4. Simplified scheme accounting for intramolecular PEnT processes involved in the fine-tuning of the lifetime of the pivotal ^{3}MLCT lowest thexi state (T_1) of **P** within **P**~**A** and **P-(*θ*)-A** assemblies, and following photoinduced formation of the **P**-centered ^{1}MLCT excited state. ^{3}RSC refers to the **RS**-centered triplet state (T_{1A}) (**RS** = **A**), also loosely referred to as intra-ligand triplet state (^{3}IL) in the literature.

3)→ **RS** (Figs. 3 and 4) energy transfers. Roughly, (i) the remote chromophore **A** must possess its lowest-lying triplet state ($^3(\pi-\pi^*)$; T_{1A} in Fig. 4) close in energy to the T_1 state of **P** (preferably isoenergetic), (ii) the decay (whether radiative or non-radiative; path (4) in Fig. 4) of the **RS**-centered T_{1A} triplet state must be significantly slower than the decay of the **P**-centered T_1 (in particular for the phosphorescence) and (iii), the intercomponent EnT (path (3) forward and backward rate; Fig. 4) must be larger than the decay rates of both triplets (T_1 and T_{1A}). Clearly coming within the fine-tuning approach of the features of **P**, the concept is actually plural in its developments and implementations. Originally [75] perfected for covalent assemblies linked by "saturated" insulating spacers (such as – flexible – hydrocarbon tethers) that is, genuine **P**~**A** supermolecular assemblies (PMDs of type (A) in Section 1.2.3) [118], the concept was later demonstrated also to be workable with linkers capable of mediating substantial electronic coupling such as ethynylene connectors [119]. It remains nonetheless true that, in this case, the connector also serves as a π-extending group [120] known to perturb excited-state features of ***P** (Section 1.4.4.1). The behavior of the overall assembly is therefore worth describing as a fairly coupled supermolecule of type (B) (cf. Section 1.2.3). Even in the case of compact assemblies deprived of true *spacer* (the **P** and **RS** are directly bonded) but showing a dihedral angle (*θ*) between sub-systems formally functioning as *such* [121] (refer to the **P-(*θ*)-RS** borderline case of interest evoked in Section 1.2.3), **RS** can act as a temporary energy reservoir even though it is not involved in a reversible EnT. For such electronically closely coupled, spatially compact and semi-rigid **P-(*θ*)-A** two-component (super)molecules, direct intersystem crossing (isc$_{\mathbf{P-RS}}$) between the lowest-lying MLCT singlet state of **P** (S_1) and the triplet-state of **A** (T_{1A}) has been demonstrated (Fig. 4). Accordingly, the quantum yield for the intra-photosensitizer isc$_\mathbf{P}$ between ^{1}MLCT and ^{3}MLCT states ($\Phi_{isc,\mathbf{P}}$ in Fig. 4) usually assumed to be unity is, in this special case, significantly smaller and typically only *ca.* 0.7 [121]. In other words, close coupling (either spatial or electronic) allows part (*ca.* 30%) of the energy attached to the ^{1}MLCT state of ***P** to be directly transferred to the remote T_{1A} energy reservoir, so bypassing the lowest thexi state of the photosensitizer. Energy stored in the form of the T_{1A} state of the **RS** is finally returned to **P** by populating its T_1 state (pathway (3) in Fig. 4, taken forward to **P** [122]). As a result of the delayed population of T_1 (in addition to usual –direct – population from the higher-lying ^{1}MLCT state), the lifetime of the lowest thexi state of ***P** is markedly increased [121,123]. The fact that this behavior is observed in such a closely coupled assembly is indicative of one of the basic feature of triplet states, namely their *locally excited states* nature (LES; Fig. 2), moreover capable of exhibiting rather strong electronic coupling without getting denaturized [124].

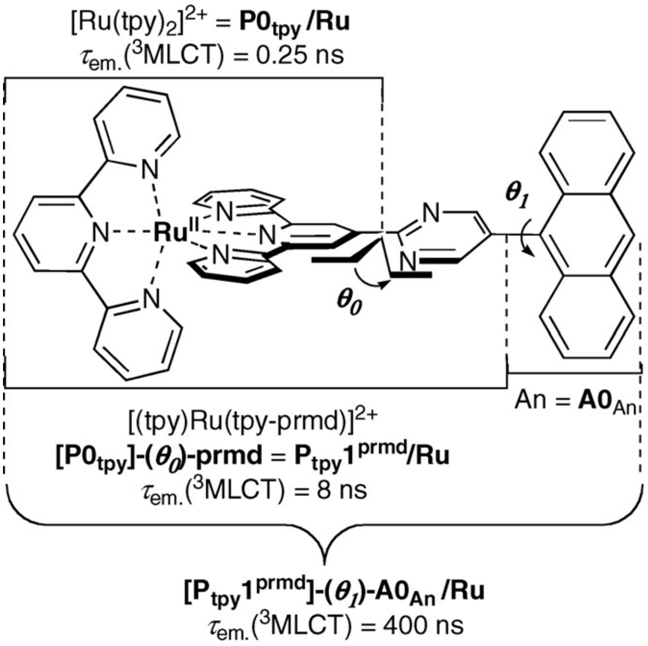

Fig. 5. Salient features of a semi-rigid fairly coupled **P-(*θ*)-A** supermolecule designed to extend the lifetime of the lowest thexi state of the $\mathbf{P0_{tpy}/Ru}$ core (that is, $[Ru(tpy)_2]^{2+}$ luminophore) [125a].

Finally, one of the most promising means to prolong the lifetime of the lowest thexi state of a given **P0** core was to combine the approach based on extended electron delocalization of primary ligand(s) (**P1**) [125] (Section 1.4.4.1) with the multi-chromophoric approach based on the use of remote energy reservoir(s) (**P**~**A**) [77,110]. In the illustrative case of trans-meridional bis-terdentate Ru(II)-based photosensitizers (i.e. $\mathbf{P0_{tpy}/Ru}$), the **P0** is first substituted by a π-extending and π-accepting decoration (namely the 2-pyrimidinyl group, prmd; cf. Section 1.4.4.1) and the resulting **P1** type of chromophore (i.e. $\mathbf{P_{tpy}1^{prmd}}$) is subsequently linked to a suitable **RS** as energy acceptor **A0** (namely an anthracene unit, denoted $\mathbf{A0_{An}}$; see Fig. 1) to give the $\mathbf{P_{tpy}1^{prmd}\text{-}(\theta_1)\text{-}A0_{An}}$ assembly (Fig. 5). Thereby embedded within a fairly coupled semi-rigid $\mathbf{P\text{-}(\theta_1)\text{-}RS}$ supermolecules of type B (as defined in Section 1.2.3), the $\mathbf{P0_{tpy}/Ru}$ luminophore ($\tau_{em} \approx 0.25$ ns) has its emission lifetime increased by a factor of 1600 (up to 400 ns [123,125a]) [126]. Moreover, from a more general viewpoint, this combined approach has the great asset over the original multichromophoric approach based on flexible linkers [75,118] to allow better control over the rigid molecular geometry, which is of paramount importance for PMDs meant to perform directional PET and PEnT. Intramolecular steric hindrance about the intercomponent linkage results in a geometrical decoupling (represented by torsion angle θ_1) correlated with a partial electronic decoupling of the **P** and **RS** subsystems. Torsion angle θ_1 thus ensures the preservation of key electronic features of the components (see Section 1.2.3), therefore virtually playing the role of a spacer within the compact semi-rigid supermolecule [77,110].

*1.5. Assessing the impact of conformational changes on photoinduced processes within semi-rigid photosensitizer–acceptor (**P–A**) inorganic assemblies*

Throughout Section 1 various backgrounds involved in the plural field of supramolecular (inorganic) photochemistry have been outlined, with a particular focus on the implementation for artificial photosynthesis. At each stage, possible ways for structural properties (including conformation) and electronic properties (including photophysics and photochemistry) to interplay have been highlighted. Among semi-rigid and closely coupled functional architectures, intramolecular conformation is expected to be most influential with respect to the electronic working mode of supermolecules. Now, tackling in concrete terms the impact(s) of conformational fluctuations (whether thermally activated or photoinduced; cf. Section 1.3) on the electronic behavior of compact assemblies, we analyse three case studies (Sections 2–4). Emphasis is put on the consequences over both the status of the individual functional elements and their capability to interplay subsequent to absorption of light. The impact on the photophysical behavior of the primarily concerned inorganic **P** components is examined first (Section 2). Then, the impact on photoinduced processes (photochemistry) is investigated through the analysis of two special cases, which are series of photosensitizer–acceptor *putative* "dyads" (with *putative* **RS = A**) showing different degrees of compactness (Sections 3 and 4). For each illustrative case, the goal is to clarify whether the acceptor group (**A**; Fig. 1) behaves as an influential substituent (R^1 or $R^{1\theta}$) of the photosensitizer **P** (more precisely: as a substituent of the ligand(s) coordinated to the metal center) or as a remote site interacting with **P** (**P0** or **P1**), the intercomponent electronic coupling being tuned by intervening torsion angle θ (Fig. 1). In other words, the question is to determine whether we are dealing with *large* molecules fitting a *delocalized description* of their electronic/photophysical properties (denoted as $\mathbf{P(\theta)^A}$) or with multicomponent assemblies fitting a *localized description* and referred to as *supermolecules* (namely dyads $\mathbf{P\text{-}(\theta)\text{-}A}$), respectively (see Section 1.2.3). To avoid misleading issues related to the solvent dependence of dynamic structural changes such as planarization [56], comparisons were made between photoinduced behavior investigated under the same experimental conditions [56].

2. Case study A. Light-induced structural changes *around* the luminophoric core P0: the impact of planarization of phenyl decorations within P1

$[Ru(bpy)_3]^{2+}$ (denoted $\mathbf{P0_{bpy}/Ru}$) and $[Ru(tpy)_2]^{2+}$ (denoted $\mathbf{P0_{tpy}/Ru}$) are prototype photosensitizers in the field of supramolecular inorganic photochemistry even though they display sharply different photophysical features. As previously mentioned, exploiting the appealing geometrical features of $\mathbf{P0_{tpy}/Ru}$ (namely achirality and overall axial symmetry) [86] to build PMDs is not that straightforward because of the poor photophysical properties of the basic photosensitizer. Much effort has been devoted during the last two decades to improve both the absorption and emission properties of $\mathbf{P0_{tpy}/Ru}$, including the lifetime of its lowest thexi state (see Section 1.4). To this end, decorating the $\mathbf{P0_{tpy}/Ru}$ core with aryl groups was soon proposed and more precisely, phenyl-substitution of tpy ligands at either or both (4, 4″) and 4′ position(s) [127,128]. Of particular interest for PMDs designed for photoinduced charge separation are those $\mathbf{P0_{tpy}}$-based photosensitizers bearing aryl fragments along the main molecular axis (that is, appended at the 4′ position of tpy ligands) [86]. These semi-rigid complex photosensitizers display some conformational degrees of freedom within their decoration layer (aryl substituents are of the $R^{1\theta}$ type; cf. Fig. 1) and are therefore of interest here, as the first case study. The series of complexes examined (**0-Ru**, **1-Ru**, **0-Os** and **1-Os**) is depicted in Fig. 6.

With respect to the nomenclature adopted to describe various functional assemblies, the tilt angle is not explicitly mentioned if it is not functioning as an *intercomponent* spacer with respect to intramolecular electronic coupling (cf. Fig. 5). Here, phenyl decorations obviously have the status of $R^{1\theta}$ substituents with respect to the $\mathbf{P0_{tpy}/M}$ core (see below). Hence, the $\mathbf{P0_{tpy}(\boldsymbol{\theta_0})^{ph}/M}$ large photosensitizers (**1-Ru** and **1-Os**; Fig. 6) are referred to as **P1**/**M** type of photosensitizers, namely $\mathbf{P_{tpy}1^{ph}/M}$ (see Fig. 1 and Section 1.2.3).

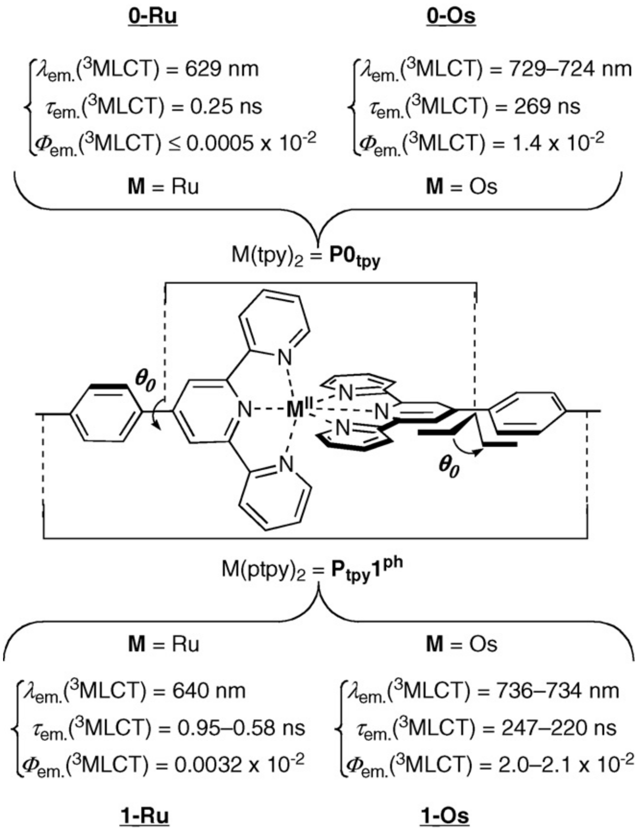

Fig. 6. Planarization (about $\boldsymbol{\theta_0}$) within the decoration layer of the $\mathbf{P0_{tpy}}$ core. The principal photophysical features of $\mathbf{P0_{tpy}/M}$ luminophores are presented together with their related phenyl decorated derivatives, $\mathbf{P_{tpy}1^{ph}/M}$. Note that the reported data actually correspond to closely related tolyl-substituted ($R^{1\theta}$) photosensitizers. Emission data recorded from deaerated nitrile solutions (**0-Ru**: [84,86,115c,129]/**0-Os**: [88,115a,129]/**1-Ru**: [86,115a,115c,129]/**1-Os**: [86,115c,129]). For nomenclature, refer to Figs. 1 and 2.

Regarding the electronic features of the photosensitizers, in addition to increasing absorption in the UV range, appending phenyl groups to $\mathbf{P0_{tpy}}$ to form the $\mathbf{P_{tpy}1^{ph}}$ chromophores also results in a significant enhancement of the extinction coefficient (ε) of the MLCT transition(s). In the case of the Ru(II) complexes, spin allowed ^{1}MLCT transitions are shifted to lower energy (from 475 nm for **0-Ru** to 490 nm for **1-Ru**) with extinction coefficients more than twice as large (from $1.48 \times 10^4\,M^{-1}\,cm^{-1}$ to $3.39 \times 10^4\,M^{-1}\,cm^{-1}$, respectively). In the case of Os(II) complexes, the same trends are observed: a bathochromic shift of *ca.* $560\,cm^{-1}$ (from 477 nm for **0-Os** to 490 nm for **1-Os**) and an hyperchromic change of *ca.* 60% (from $\varepsilon = 1.74 \times 10^4\,M^{-1}\,cm^{-1}$ to $\varepsilon = 3.01 \times 10^4\,M^{-1}\,cm^{-1}$, respectively). Similarly, the supplementary bands corresponding to formally spin-forbidden ^{3}MLCT transitions are also red-shifted and intensities increased by 60% on average: from 632 nm ($\varepsilon = 0.43 \times 10^4\,M^{-1}\,cm^{-1}$) and 658 nm ($\varepsilon = 0.47 \times 10^4\,M^{-1}\,cm^{-1}$) for **0-Os** to 645 nm ($\varepsilon = 0.67 \times 10^4\,M^{-1}\,cm^{-1}$) and 668 nm ($\varepsilon = 0.77 \times 10^4\,M^{-1}\,cm^{-1}$) for **1-Os**.

The impact of the phenyl substitution on the absorption features of the $\mathbf{P0_{tpy}}$ chromophoric core is in line with electronic effects obtained by the fine-tuning of related $\mathbf{P0_{bpy}/Ru}$ and $\mathbf{P0_{phen}/Ru}$

cores with phenyl decorations [130]. Moreover, the electronic changes are highly informative on the actual role of the $R^{1\theta}$ groups. Indeed, with respect to the ^{1}MLCT transitions, the substantial increase of extinction coefficient (ε) can be related to a "transfer term", which is itself proportional to an increase of the effective transfer length (effective electron-transfer distance) involved in the MLCT [89a,131–133]. In that sense, a hyperchromic effect is indicative of the π-extending role of the phenyl fragments with respect to CT [89b,134]. The decrease of the energy of the LUMO is correlated with extended π-conjugation, hence the observed red-shift (bathochromic effect) of the MLCT absorption with respect to $\mathbf{P0_{tpy}/M}$ parents. The point is that the π-extending role revealed by absorption features is actually related to the instantaneous – Franck–Condon prepared – conformation of **P1** chromophores, frozen in the geometry of the ground state (and characterized by θ_0; Fig. 6). As explained in Section 1.3, it is expected that the semi-rigid structure will relax towards (co-)planarity subsequent to charge redistribution (MLCT state formation). Emission is therefore expected to originate from a *planarized* lowest thexi state characterized by a sizably different intraligand conformation ($^*\theta_0 < \theta_0$) and namely, a greater extension of π-conjugation. In other words, the emission energy is anticipated to be smaller than estimates derived from known correlations between ground-state and excited-state properties.

Phenyl substitution has some intriguing aspects within the framework of an early and thorough analysis of substituent effects on the $\mathbf{P0_{tpy}/Ru}$ prototype. In 1995, Maestri et al. [84] investigated a large series of $\mathbf{P_{tpy}1^{R}/Ru}$ complexes. For a wide range of electron-donating and accepting decorations of $\mathbf{P0_{tpy}/Ru}$, they found correlations between electrochemical redox potentials, the Hammett substituent parameter (σ) and the emission energies originating from ^{3}MLCT level. However, they noticed a discrepancy for the π-extending phenyl substituent, which induces a larger red-shift of the emission energy than would be expected simply on the basis of its σ value (virtually the same as that of proton). At that time, they ascribed this deviation indicative of a stabilized emissive state compared with the electrochemical expectations to some structural reorganization intervening in the excited state leading to $^*\theta_0 \neq \theta_0$ (Fig. 6). More precisely, they hypothesized a relaxation (conformational change) towards a structure which stabilizes the charge separation created by light excitation, without giving further indication regarding the rotation tendency: twisting ($\theta_0 < {}^*\theta_0$) versus planarization ($\theta_0 > {}^*\theta_0$)? (cf. Section 1.3). Of note, they also inferred that even if the phenyl substituent is solely a π-*extending* group (rather than π-*accepting* like the pyrimidinyl fragment; cf. Section 1.4.4.1), it can certainly behave as an electron-accepting moiety in the excited-state, when the ^{3}MLCT (lowest thexi) state is formed [84].

A few years before this extensive experimental work was performed, Calzaferri and co-workers [135] had carried out extended Hückel calculations on the phenyl-decorated $\mathbf{P0_{tpy}/M}$ chromophore at the 4′ position of the tpy ligands that is, $\mathbf{P_{tpy}1^{Ph}/M}$ species (**1-Ru** and **1-Os** in Fig. 6). Insights gained from these molecular orbital studies clearly indicated that intra-ligand *planarization* ($\theta_0 > {}^*\theta_0$) was the excited-state structural relaxation expected to occur subsequent to MLCT state formation. These issues were further substantiated only very recently in the case of $\mathbf{P_{tpy}1^{ph}/Os}$ embedded within dyads (cf. see Section 4, case study C) at both the experimental level (ultrafast spectroscopy [115a]) and the theoretical level (from first principle: DFT calculations [114,115b]). Of note, it was found that steric hindrance between the four hydrogen atoms about interannular linkages is not completely withdrawn so that full coplanarity is not reached ($\theta_0 > {}^*\theta_0 \neq 0$), hence the interest of replacing the phenyl moiety with other sterically less demanding aryl extensions.

Actually, the first definitive demonstration of excited-state planarization of peripheral phenyl substituents came from the study of the other prototypic photosensitizer, namely $\mathbf{P0_{bpy}/Ru}$. Indeed, parallel to studies devoted to phenyl-substituted $\mathbf{P0_{tpy}/Ru}$ photosensitizers, McCusker and co-workers undertook a comprehensive study to rationalize the intriguing photophysical behavior of various phenyl-decorated $\mathbf{P0_{bpy}/Ru}$ derivatives. From 1997, combining experimental [136] and theoretical [137] approaches, they provided compelling evidence to support the occurrence of excited-state planarization. Finally, they investigated these model photosensitizers using ultrafast transient absorption spectroscopy and could show that excited-state conformational relaxation takes place within *ca.* 2 ps (picoseconds) in the case of the phenyl-decorated $\mathbf{P0_{bpy}/Ru}$ complexes [138] and involves the ^{3}MLCT lowest thexi state, given that intersystem crossing occurs within *ca.* 50 fs (femtoseconds) [11].

In Fig. 6 are listed the emission quantum yields (Φ_{em}) and lifetimes (τ_{em}) of $\mathbf{P0_{tpy}/M}$ cores and related $\mathbf{P_{tpy}1^{Ph}/M}$ photosensitizers. Clearly, in addition to remarkably increasing photosensitizer absorption cross-sections (light-harvesting elements of integrated antenna), phenyl substituents also significantly improve their emission properties [139], including lifetimes of the lowest thexi states. The detrimental contribution of *planarization,* as a structural reorganization, further contributing to radiationless deactivation [140], is more than compensated by the correlated reduction of the Franck–Condon factor [87,100]. With the beneficial impact of enhanced electron delocalization on the photophysical features in mind (see Section 1.4.4.1), it follows that the substantial photophysical improvements noticed in passing from naked to phenyl-decorated luminophores, in part, result from unexpected excited-state planarization. In other words, excited-state conformational relaxation towards intra-ligand coplanarity (that is, *planarization*) further contributes to improving the photophysical features of the photosensitizers (whether $\mathbf{P0_{tpy}/M}$ or $\mathbf{P0_{bpy}/M}$) *to a greater degree than originally expected (or planned) from the decoration of these cores with phenyl substituents* [84,130,141].

Brought together, these observations highlight the beneficial impact of *phenyl planarization* on the photophysical features of **P**, in the context defined in the present review. Moreover, *planarization* appears to be a widespread phenomenon as far as aryl extensions involved in CT processes within semi-rigid architectures are concerned. To some extent, this behavior also illustrates the fact that the chromophore entity, which absorbs light, is not necessarily identical to the luminophore entity which re-emits light, even though these two entities are formally the same, namely the photosensitizer **P**.

3. Case study B. Conformational gating of the photophysical/photochemical behavior of the luminophore within P0-A compact assemblies

Linking functional groups as putative full components to the complex photosensitizer (**P**), is the next step towards multifunctional assemblies like PMDs. Whether the added subunit is directly connected to **P** or linked via an intervening spacer, it is expected that planarization will occur as far as aryl fragments are involved in charge redistribution. In this section, the case of compact assemblies made up of an acceptor group (**A**) covalently tied to **P** without a spacing molecular fragment but with a tilt angle (θ_{0A}), is examined (Fig. 7). The question addressed here for each member of the series of complexes is whether we are dealing with a $\mathbf{P0_{L}\text{-}(\boldsymbol{\theta}_{0A})\text{-}A}$ supermolecular dyad species or with a $\mathbf{P_{L}1^{A}}$ large photosensitizer (see Section 1.2.3). In doing so, the aim is to delineate the role of the intramolecular conformation (θ_{0A}) in this determination ($\mathbf{P0_{L}\text{-}(\boldsymbol{\theta}_{0A})\text{-}A}$ versus $\mathbf{P_{L}1^{A}}$).

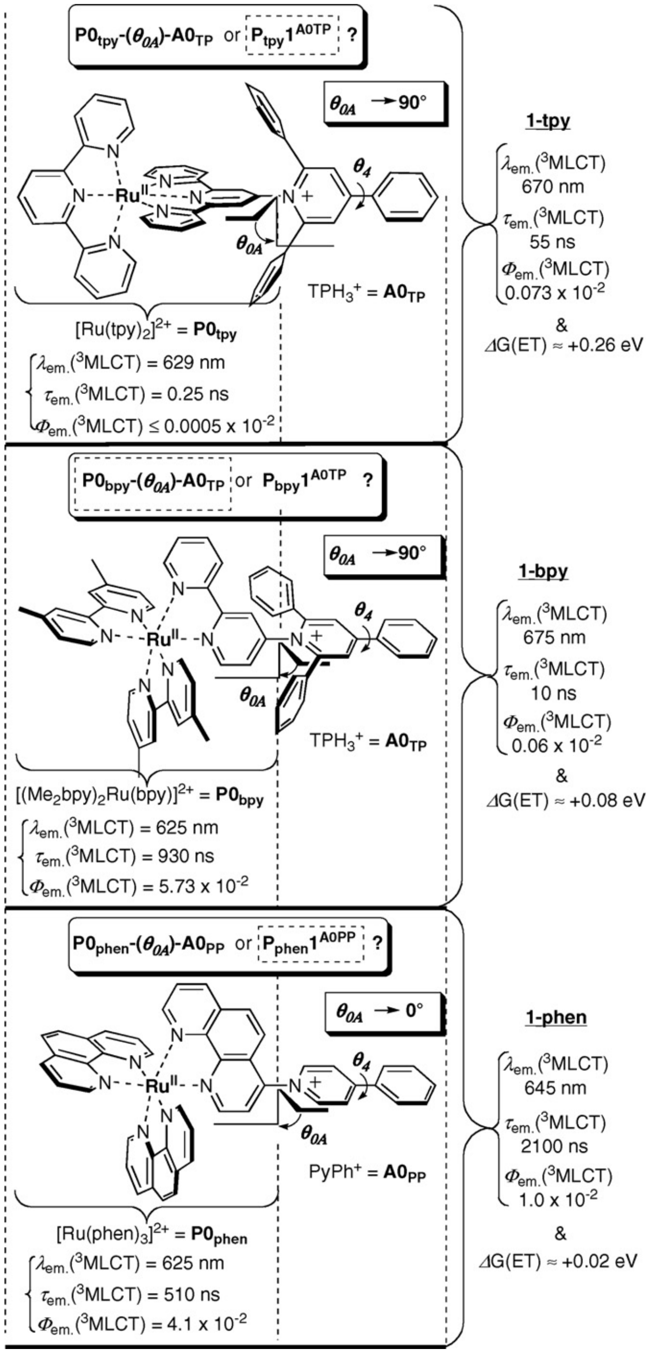

Fig. 7. Conformational gating of the photophysical/photochemical behavior of the luminophore; the status of **1-tpy** [115c], **1-bpy** [45] and **1-phen** [45,142] compact assemblies: **P0-(θ_{0A})-A/Ru** supermolecules (see Section 1.2.3) or **$P0^A$/Ru** (that is, **P1/Ru** also denoted **P0(θ_{0A})^A/Ru**) large molecules? Room-temperature photophysical features (recorded in deaerated MeCN solution) of selected Ru-based compounds together with related bare **$P0_L$** reference photosensitizers [143].

Clearly, *planarization* is expected with aryl groups other than the phenyl substituent, all the more so if they are not only a π-extending but also a π-accepting group such as the pyrimidinyl extension (Section 1.4.4) or the currently used pyridinium ring electron acceptor. Indeed, photoinduced planarization is well established for pyridinium derivatives [7], whether based on mixed pyridyl-carbonyl complexes of Re(I) [144] or based on Ru(II) polypyridyl complexes [114,145,146]. In contrast to **$P_{tpy}1^{ph}$/Ru** (**1-Ru** in Fig. 6), however, there is a pronounced steric congestion about the linkage between the pyridinium ring (central to the triphenylpyridinio moiety, TPH_3^+; Fig. 7) and the **$P0_L$** core within **1-tpy** and **1-bpy**. As a result of the presence of bulky phenyl substituents at either side of the $N_{pyridinio}$ atom, the θ_{0A} value approaches 90° in both cases [45,111,114,115,147,148]. This structural feature is usually referred to as *geometrical decoupling* [111,114,115]. For **1-phen**, there is no such large intramolecular hindrance but only the usual small repulsion between the hydrogen atoms *ortho* to the interannular bond, as in **1-Ru**. Thus, θ_{0A} about the pyridinium-phen linkage approaches 0° within **1-phen** in the ground state (θ_{0A} actually amounts to *ca.* 25° [142]) [111].

Another noticeable difference between the three members of the series stems from the capability of the pyridinium, as a redox-active subsystem, to potentially act as a partner for photoexcited **P**. By combining electrochemical and low-temperature emission data derived from the photoactive species, one can generate *estimates* [88] of the excited-state redox properties of ***P** embedded within its specific molecular landscape, hence assessing the driving force (ΔG(ET)) for photoinduced intercomponent ET (towards charge separation) [54,88,149–151]. While clearly endergonic (>0) for **1-tpy**, ΔG(ET) is borderline (roughly isoenergetic or barely endergonic) for **1-bpy** and **1-phen** (cf. Fig. 7). Changes in the intraligand torsion angles, θ_{0A} or θ_4 (attached to the almost freely rotating phenyl terminus at the position 4 of pyridinium; Fig. 7), are likely to impact the redox properties of the pyridinium: the smaller the twist angle the greater the electron-acceptor features [45,115a,146,152]. Excited-state planarization is therefore anticipated to reinforce the electron-withdrawing capability of the pyridinium moiety [142] even though this latter is supposed to be reduced when the (ML)CT or CS state is formed. This synergistic (or feed-back) effect correlated with a change of the driving force makes the solutions to various thermodynamic issues, related to excited-state properties including, for example, ΔG(ET), rather approximate.

Lastly, neither TPH_3^+ (**$A0_{TP}$**) nor the *p*-phenyl-pyridinium $PyPh^+$ (**$A0_{PP}$**; Fig. 7) can play the role of an energy acceptor with respect to **$P0_L$/Ru** as their triplet energies (revealed by low-temperature phosphorescence of acceptor models at *ca.* 450 nm [115b,115d]) lie well above that of the corresponding ^{3}MLCT state of **$P0_L$/Ru** units embedded within their respective assemblies (λ_{em}(**$P0_{tpy}$**) = 670 nm, λ_{em}(**$P0_{bpy}$**) = 675 nm and λ_{em}(**$P0_{phen}$**) = 645 nm at room temperature in deaerated acetonitrile). Moreover, **$A0_{TP}$** and **$A0_{PP}$** are both UV-absorbing fragments while **$P0_L$/Ru** complexes are NIR emitters. Therefore, **P0/Ru** → **A0** energy transfer cannot explain the quenching of the luminescence of **$P0_{bpy}$** within **1-bpy**. Neither can an energy equilibration process be proposed to account for the increased emission lifetime of both **$P0_{tpy}$** within **1-tpy** and **$P0_{phen}$** within **1-phen** as compared with relevant reference isolated photosensitizers [45].

Analysis of the absorption features of **1-tpy**, reveals a large hyperchromic effect accompanied with a bathochromic shift of the ^{1}MLCT transition when compared with the reference **$P0_{tpy}$/Ru** [111]. As previously (case study A; **1-Ru** with respect to **0-Ru**), these changes are indicative of spatially extended CT electronic transitions. However, because of the persistent intramolecular geometrical decoupling about θ_{0A}, mentioned above, impacts on ε and absorption energy are no longer related to a further extension of π-conjugation but are rather ascribed to the through sigma-bond mediated electron-withdrawing effect of the positively charged $N_{pyridinio}$ atom (inductive contribution (−*I*), essentially). At one and the same time, the π* ligand-centered LUMO orbital is stabilized and the ^{3}MLCT–^{3}MC energy gap enlarged. This translates into the observed red shift of the emission (reduced ^{3}MLCT–GS energy gap) and a remarkably increased emission lifetime (*ca.* 200-fold increased compared with parent **$P0_{tpy}$/Ru**; Fig. 7), respectively (see Section 1.4). With respect to the photophysical behavior of **1-tpy**, the possible minor contribution of the intervening electron-delocalization effect associated with a slight excited-state planarization about θ_{0A} cannot be strictly ruled out, even though torsional motion is largely impeded. Lastly, bearing in mind that intramolecular PET from ***P0$_{tpy}$/Ru** to TPH_3^+ is, by far, thermodynamically forbidden, **1-tpy** is worth considering as a *large photosensitizer* (**P$_{tpy}$1^{TPH3}/Ru**) that is, a made-in-one-piece luminophore at the electronic level.

With respect to **1-bpy**, intramolecular geometrical constraints are virtually the same as for **1-tpy** (geometrical decoupling). The same issues also hold for the electronic perturbation of the **P0$_{bpy}$/Ru** chromophore by the $N_{pyridinio}$ atom of TPH_3^+, even though a splitting of the ^{1}MLCT absorption band is observed [45] instead of the equivalent hyperchromic effect previously noticed [111]. The point is that **P0$_{bpy}$/Ru** is a significantly better electron-donating agent in the excited state (E(III/II*)) than **P0$_{tpy}$/Ru**: −0.92 V versus −0.76 V versus SCE, respectively. Most importantly, this trend is retained in related complexes despite the detrimental electronic impact of the appended TPH_3^+: E(III/II*) = −0.68 V for **P0$_{bpy}$/Ru** within **1-bpy** versus E(III/II*) = −0.51 V for **P0$_{tpy}$/Ru** within **1-tpy**. Consequently, ΔG(ET) is switched from unfavorable (case of **1-tpy**) to borderline (case of **1-bpy**), thus becoming compatible with the occurrence of a poorly efficient intramolecular PET with CS state formation that is, an *intercomponent* process indicative of a *supermolecular* behavior (see Section 1.2.3). At one and the same time, TPH_3^+ is a *substituent* of **P0$_{bpy}$/Ru** (large molecule behavior) and a *partner* of ***P0$_{bpy}$/Ru** (supermolecule behavior). The overall behavior is actually that of a compact **P0-(θ_{0A})-A** *supermolecule*, as revealed by the quenching of the phosphorescence of **P0$_{bpy}$/Ru** within **1-bpy** most likely resulting from intercomponent ET (path 3 in Figs. 3 and 4) [45].

With respect to **1-phen**, the energetics are essentially the same as for **1-bpy** that is, borderline driving force for intramolecular PET. On the other hand, there is no geometrical decoupling about θ_{0A}, so that planarization is not impeded in the lowest thexi state, contrary to **1-bpy**. The photophysical behavior of **1-phen** is sharply different from that of **1-bpy** insofar as the lifetime of the emission originating from the ^{3}MLCT lowest thexi state is dramatically increased compared with **P0$_{phen}$/Ru** parent luminophore [142] (Fig. 7) instead of getting dramatically shortened, like for **1-bpy**. This observation is fully consistent with the development of an extended π-*delocalization* over the planarized domain of the phen-$PyPh^+$ ligand ($^*\theta_{0A} \approx 0^\circ$) in the lowest thexi state. As explained in Section 1.4.4.1, this delocalization contributes to diminishing the vibrational overlap between the lowest thexi state and the final ground state, hence reducing the efficiency of non-radiative decay accordingly. Thereby, in the case of **1-phen**, the photo-promoted electron is finally *delocalized* over the whole planarized phen-$PyPh^+$ "super-ligand" giving rise to a "super-MLCT" emitting state [45,142], rather than being *transferred* to the pyridinium center (CS state formation) as in the case of **1-bpy**. In other words, the whole **1-phen** complex is worth considering as a *large photosensitizer* (**P$_{phen}$1^{PyPh}/Ru**) fitting a delocalized description of its electronic/photophysical features.

The overall picture we get from the cross comparison of the respective photophysical behavior of **1-tpy**, **1-bpy** and **1-phen** is as follows.

- Firstly, at the functional level, the twist angle θ_{0A} is not relevant as a spacer in the two following cases: (i) for **1-tpy**, because the appended TPH_3^+ moiety is not a full component of the bipartite molecule but only a decoration of the **P0$_{tpy}$/Ru** core (TPH_3^+ is a locked $R^{1\theta}$ substituent that is, a (−I) R^1 substituent; Fig. 1); (ii) for **1-phen**, because this torsion angle lies within the phen-$PyPh^+$ "super-ligand" and merely vanishes in the planarized lowest thexi state since $PyPh^+$ is a (−I, −M) $R^{1\theta}$ substituent (Fig. 1) of the **P0$_{phen}$/Ru** core.
- Secondly, brought together, observations concerning **1-bpy** and **1-phen** indicate that, as far as π–π interaction is concerned, which has by far the largest contribution to intramolecular electronic communication, geometrical decoupling is rather efficient to produce electronic decoupling, including within closely coupled and compact assemblies. This issue is in line with literature reports concerning other less compact assemblies [1,111,114,115,117,147,153–159].

All things being equal between **1-bpy** and **1-phen** (namely, **P0$_{bpy}$/P0$_{phen}$** with respect to **A0$_{TP}$/A0$_{PP}$**) in particular regarding the borderline driving force for intramolecular PET, it is shown here that changing a conformational parameter (such as θ_{0A}) that is, the electronic coupling between **P0** and **A**, merely changes the status of the whole molecule from that of a supermolecule (case of **1-bpy**) to that of a large molecule (case of **1-phen**). The emission properties are switched accordingly from non-emissive for **1-bpy** (due to intramolecular oxidative quenching of ***P** and CS state formation) to increased emission lifetime for **1-phen** (due to enhanced excited-state delocalization and super-^{3}MLCT state formation).

4. Case study C. Conformational gating of intercomponent photoinduced processes within P1-A assemblies

In this section, the series of four complexes depicted in Fig. 8 is examined. These assemblies are made up of an Os(II) bis-tpy complex (**P0$_{tpy}$/Os**) linked via an aryl moiety to a triaryl-pyridinio group (TP^+) [115a].

First of all, similar to the $R^{1\theta}$ phenyl substituent of the **P0$_{tpy}$/M** core (Fig. 1) investigated in Section 2, aryl moieties (whether phenyl, tolyl or xylyl) subject to planarization fully partake in the photosensitizer component [86,134]. **P0$_{tpy}$-(θ_0)-aryl/M** is a single electronic entity therefore worth referring to as **P$_{tpy}$1^{aryl}/M** (actually **P$_{tpy}$(θ_0)1^{aryl}/M** in the ground state giving ***P$_{tpy}$(*θ_0)1^{aryl}/M** in the lowest thexi state; see Section 2). In other words, θ_0 is no longer a determining twist angle while θ_1 possibly functions as a spacer for the complexes of the present case study (Fig. 8).

Two parameters are to be varied here: (i) the level of restriction for torsional motion about θ_1 and (ii), the driving force for photoinduced intramolecular ET. Replacing the intervening phenyl moiety between **P0$_{tpy}$/Os** and the TP^+ group with a xylyl fragment allows a modifying structural factor (i). Thereby, the steric encumbrance about the linkage attached to θ_1 is changed from "two hydrogens – two phenyls" (*restrained* torsional motion; case of **2-Os** and **4-Os**) to "two methyls – two phenyls" (*constrained* or even *locked* torsional motion; case of **3-Os** and **5-Os**), respectively. On the other hand, modulating the thermodynamic factor (ii) goes through the nitro-substitution of the triaryl-pyridinio moiety ($TPH_3^+ \rightarrow TPH_2(NO_2)^+$; Fig. 8) to improve (strengthen) the electron-accepting capability of TP^+ as a *potential* remote site (**RS = A**) and redox partner of ***P**.

Noteworthy, the four assemblies show essentially the same θ_1 twist angle (ranging between 85° and 90°) as judged from crystallographic data [111,115a] that is, they apparently have virtually the same geometrical decoupling about θ_1 in the ground state, regardless of the harshness of intramolecular steric hindrance. However, via thermally activated torsional motion, twist angle θ_1 experiences a wider angular range within *restrained* **2-Os** and **4-Os** than within sterically *constrained* **3-Os** and **5-Os**. The same issues obviously hold for excited-state photoinduced planarization. With the angular dependence of electronic coupling [111,114,115,117,147,153–159] in mind, it follows that torsional fluctuations of larger amplitude are therefore correlated with a greater intramolecular electronic

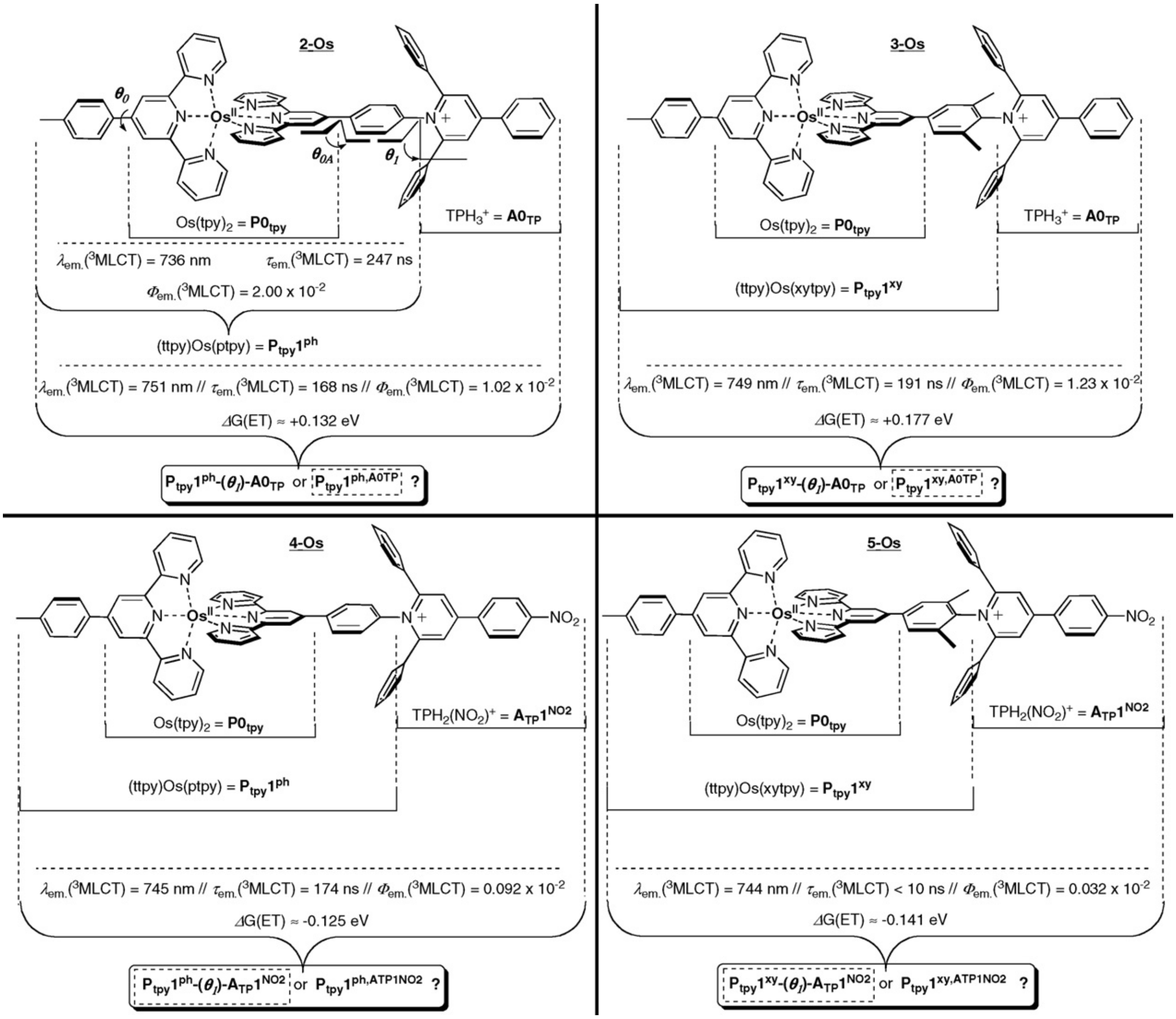

Fig. 8. Conformational gating of intercomponent photoinduced processes; the status of **2-Os**, **3-Os**, **4-Os** and **5-Os** assemblies: **P1-(θ_1)-A** supermolecules or **P1^{A}** larges molecules? [143]. Room-temperature photophysical features (recorded in MeCN deaerated solution) of selected Os-based compounds [115a].

coupling in the average (case of **2-Os** and **4-Os**) than torsional fluctuations of smaller amplitude like those allowed within constrained **3-Os** and **5-Os**. Thereby, despite formally the same geometrical decoupling in the ground state, intramolecular electronic coupling is greater within **2-Os** and **4-Os** than within **3-Os** and **5-Os**. To summarize, the level of steric restriction about θ_1 impacts both thermally activated torsional fluctuations and photoinduced planarization, hence the magnitude of the intramolecular electronic coupling.

Conversely to the previous case study (Section 3), no sizable change in the absorption features attached to ^{1}MLCT and ^{3}MLCT transitions could be found when comparing the electronic spectra of the various members of the series [115a]. Excited-state features are actually the more informative with respect to the extent of the intramolecular electronic perturbations of **P** by TP$^+$. The low-temperature emission spectra of various osmium-based species (**2-Os**–**5-Os**) including the bare $\mathbf{P_{tpy}1^{Ph}}$**/Os** photosensitizer (**1-Os** in Section 2) are given in Fig. 9. *Large* structural motions (typically those involving the TP$^+$ fragment about θ_1) are precluded in the rigid matrix. Also, slightly exergonic intercomponent ET processes (case of **4-Os** and **5-Os**; see below) are impeded in glass due to the endergonic contribution related to the repolarization slowdown of surrounding solvent molecules [160,161]. Examining Fig. 9,

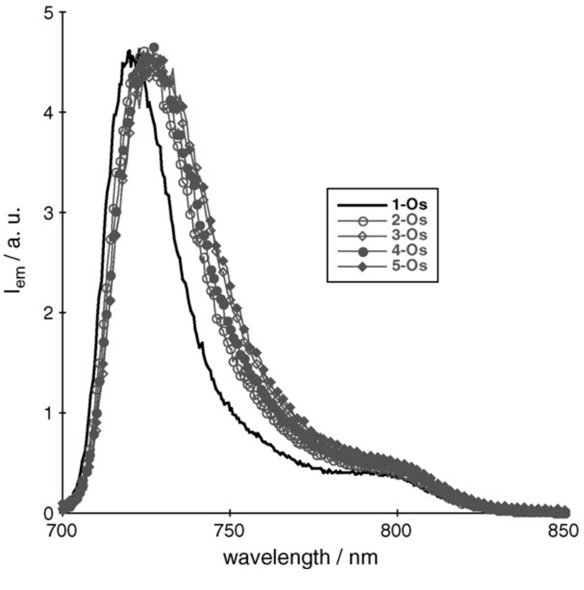

Fig. 9. Normalized low-temperature (77 K) emission spectra of **1-Os**, **2-Os**, **3-Os**, **4-Os** and **5-Os** ($\lambda_{exc.}$ = 600 nm in deaerated BuCN) [115a].

the bare complex-photosensitizer (**1-Os**) behaves differently from the other members of the series (**2-Os**–**5-Os**), which roughly have the same emission energy within experimental error regardless of the nitro substitution of TP$^+$. These observations are evidence that appending TP$^+$ to **$P_{tpy}1^{Aryl}$/Os** has a sizable permanent electronic influence on the photophysical properties of the photosensitizer. Thus, TP$^+$ primarily behaves as a *substituent* of **$P_{tpy}1^{Aryl}$/Os**. This modest substituent effect, ascribed to the presence of the positively charged $N_{\text{pyridinio}}$ atom, is also revealed by the slight anodic shift of the redox potential attached to the complex photosensitizer within the **2-Os**–**5-Os** series with respect to the one measured for **1-Os** [114,115a,115c,115d]. The fact that TP$^+$ is to some extent part of the photosensitizer is also further substantiated by time-dependent DFT calculations devoted to **2-Os**, which provided evidence for the existence of a direct optical electron transfer (that is, an electronic transition) from the metal center to the pyridinium ring of TP$^+$ lying in the UV range (at *ca.* 350 nm) [114]. The quantum yield for room-temperature emission of **2-Os**, which is half that of reference photosensitizer **1-Os**, is therefore an intrinsic feature of this **$P_{tpy}1^{Ph,TP}$/Os** *large photosensitizer*. The deviation from emission properties of **1-Os** can be ascribed to the electronic perturbation attached to TP$^+$ group as a substituent, which also provides for some supplementary radiationless deactivation pathways via torsional motion of the TP$^+$ moiety about θ_1. These issues hold for the whole series of osmium complexes. Rigidifying the molecular architecture about this linkage by adding bulky substituents (e.g. methyl groups of the xylyl fragment) indeed results in an increase of the emission quantum yield (Section 1.4.4.1) [87,162], as shown for the **3-Os** large photosensitizer compared with **2-Os** (see Fig. 8).

Interestingly, the fact that nitro-derivatization of TP$^+$ basically has virtually no additional impact *per se* on the low-temperature emission properties of photosensitizers indicates that this electron-withdrawing group essentially tunes the electronic properties of the TP$^+$ fragment. This spatially limited electronic influence is further substantiated when comparing the electrochemical features of **2-Os** and **3-Os** to those of nitro-derivatized related compounds (**4-Os** and **5-Os**). The metal-centered redox potential remains virtually the same for all four complexes (at *ca.* +0.93 V versus SCE) while the reduction potential of TP$^+$ shows an anodic shift of about 0.28 V (from *ca.* −0.92 V to *ca.* −0.64 V versus SCE) for nitro-substituted assemblies. This independence of the redox/electronic features of two parts of the same molecular assembly is a hallmark of a supramolecular behavior for the nitro species (Section 1.2.3). Although present, the *large molecule* behavior is dominated by the *supramolecular* behavior within **4-Os** and **5-Os**, which can be described as **P1-(θ_1)-A1** *dyads* (Fig. 2). These assemblies are closely coupled dyads of type (B), as defined in Section 1.2.3. Hence, the TP$^+$ *substituent also* gets the status of a *remote site* (**RS**) with respect to **$P_{tpy}1^{Aryl}$/Os**, and the NO$_2$ of TPH$_2$(NO$_2$)$^+$ is the R^2 substituent of **RS** in Fig. 1. Room-temperature photophysical behavior of **4-Os** and **5-Os** are shown to be those of supermolecules, accordingly (see below) [115a]. Finally, because of the dual nature of compact dyads of type (B), analyzing properly the photophysical behavior of **4-Os** and **5-Os** supermolecules goes through the use of **2-Os** and **3-Os** large photosensitizers of type C (respectively) as the relevant references instead of the **1-Os** photosensitizer [115a].

In fluid solution at room temperature, emission quantum yields of **4-Os** and **5-Os** dyads are roughly of the same order of magnitude that is, 9% and 2.6% of their respective **$P_{tpy}1^{Aryl,TPH3}$/Os** reference photosensitizers (**2-Os** and **3-Os**). This quenching of the luminescence arising from the ^{3}MLCT state of ***P1/Os** components (pathway (1) in Fig. 4) is firstly ascribed to intervening intramolecular photoinduced electron transfer (PET; pathway (3) in Fig. 4), leading to the formation of **P1$^+$-($^*\theta_1$)-A$^-$** charge-separated states (CSS). This explanation is further supported by favorable estimates of driving forces (exergonic ET reaction by *ca.* 0.13 eV on average; Fig. 8). A striking point, however, is that in spite of similar low emission quantum yields at room temperature, **4-Os** and **5-Os** show sharply different emission lifetimes: 174 ns and less than 10 ns, respectively. To rationalize the surprisingly long emission lifetime attached to **4-Os** and further characterize various photoinduced processes occurring within **4-Os** and **5-Os**, ultrafast transient absorption experiments were carried out (Fig. 10).

Clearly, the more diagnostic spectroscopic domain is in the NIR, between 700 and 800 nm (Fig. 10). A feature shared by the three compounds is the ultrafast rise of the absorption in the NIR domain (within *ca.* 2 ps [163]), which is ascribed to the *planarization* about θ_0/θ_{0A} of phenyl/xylyl R$^{1\theta}$ substituents of **$P0_{tpy}$/Os** within **$P_{tpy}1^{aryl}$/Os** [115a,115b] (cf. discussion in Section 2; case study A)

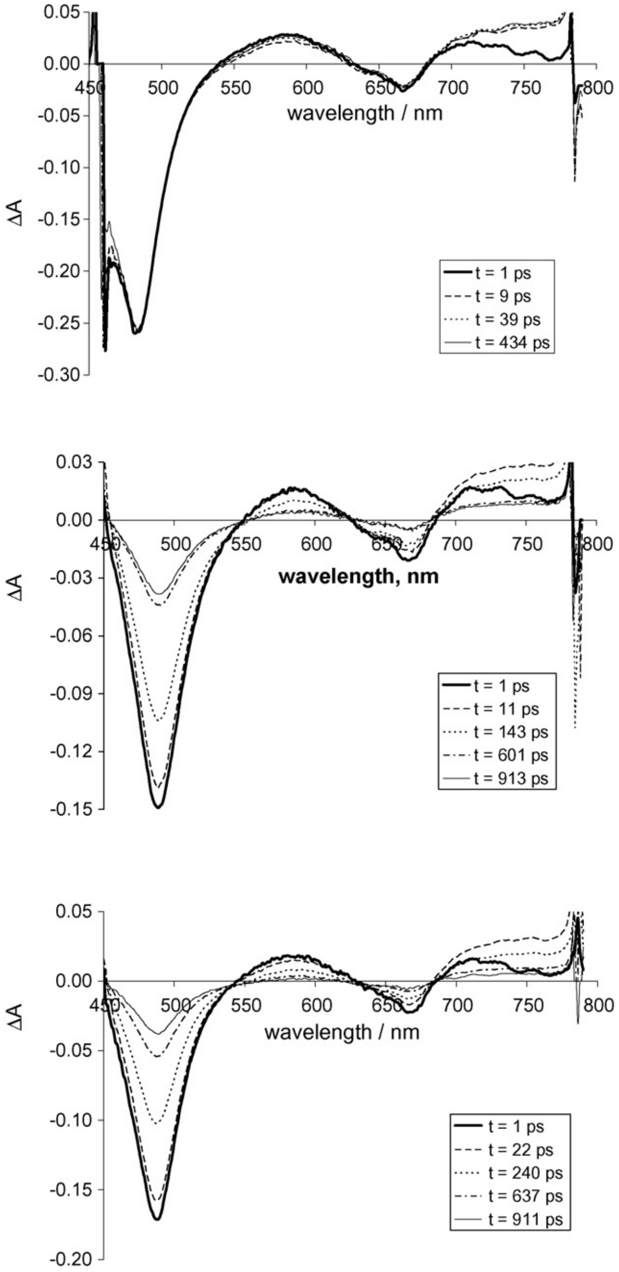

Fig. 10. Selected ultrafast differential transient absorption spectra of **3-Os**, (top), **4-Os**, (middle) and **5-Os** (bottom). $\lambda_{\text{exc.}}$ = 400 nm; deaerated MeCN solutions; first observation after 500 fs from pulse [115a].

[164]. This is the first direct evidence reported for *planarization* of aryl decorations of a **P0$_{\mathbf{tpy}}$/M** core, as the preferential structural relaxation of the lowest excited state into its thermalised conformation, corresponding to the lowest thermally equilibrated excited (thexi) state.

With respect to **3-Os**, ultrafast transient absorption spectroscopy reveals biphasic kinetics. First, there is the ultrafast component attached to the planarization within **P$_{\mathbf{tpy}}$1$^{\mathbf{aryl}}$/Os**. Then, the spectroscopic features remain unchanged in the timescale of the experiment (instrument limited to *ca.* 1000 ps), in agreement with the decay derived from emission measurements: 191 ns [115a]. These are the *photophysical* characteristics of the **3-Os** *large photosensitizer* (type C).

With respect to **5-Os**, ultrafast transient absorption spectroscopy also reveals biphasic kinetics. The first ultrafast component of *ca.* 2 ps (planarization) is followed by a slower decay of about 870 ps leading to the recovery of the ground state (Fig. 10), which is also consistent with the emission lifetime estimated to be less than 10 ns [115a]. This dramatically shortened emission lifetime as compared with reference **3-Os** is straightforwardly explained by intervening photochemistry: namely the fast formation of a CS state (within *ca.* 10^{-9} s), which does not accumulate most likely because of the peculiar influence of the nitro group [54,165].

With respect to **4-Os**, ultrafast transient absorption spectroscopy in this case reveals triphasic kinetics. The first ultrafast component (planarization) is followed by a slower decay of about 400 ps, *which does not lead to the recovery of the ground state* (Fig. 10), conversely to **5-Os**. Then, the spectroscopic features remain unchanged in the timescale of the experiment (*ca.* 1000 ps), in accordance with the decay derived from emission measurements: 174 ns [115a]. To explain the unexpected 400 ps process, intervening reversible energy transfer (equilibration) between the ^{3}MLCT thexi state (T_{1P}) of the photosensitizer and a triplet excited state (T_{1A}) located on the TP$^+$ remote site, was proposed. The existence and identity of such a T_{1A} triplet were fully established by carrying out a detailed computational study of the series of complexes as well as low-temperature phosphorescence measurements on proper nitro-derivatized model acceptors 1,2,6-triphenyl-4-*p*-nitrophenyl-pyridinium (denoted [**ph-TPH$_2$(NO$_2$)$^+$**]) and 1-*m*-xylyl-2,6-diphenyl-4-*p*-nitrophenyl-pyridinium (denoted [**xy-TPH$_2$(NO$_2$)$^+$**]) [115b]. Indeed, it was shown that there exists a T_{1A} locally excited state (LES) located on the nitrophenyl (NP) fragment embedded within TPH$_2$(NO$_2$)$^+$ acceptor units of dyads, moreover virtually isoenergetic with the T_{1P} triplet of the linked photosensitizers [115b]. The triplet located on the remote site can play the role of an energy reservoir provided suitable kinetic and thermodynamic parameters are fitted (cf. Section 1.4.4.2). The point is that EnT (equilibration) is potentially in competition with intercomponent ET (to TP$^+$ as an *electron* acceptor) as both processes involve the same ^{3}MLCT state (T_{1P}) of the photosensitizer (Fig. 11). To summarize, the 400 ps decay was assigned to the equilibration time while the luminescence lifetime could be ascribed either (i) to the quenched lifetime of the equilibrated state whose unquenched intrinsic lifetime would be rather longer in this case, or (ii) to the lifetime of the equilibrated state [115a].

Given that thermodynamics for intercomponent PET and PEnT processes are virtually the same within **4-Os** and **5-Os**, the reason why ET (that is, charge separation) appears to dominate in **5-Os** while reversible EnT (that is, equilibration) dominates in **4-Os**, at least at the early stage, remains to be clarified. It is known that torsional motions are correlated with fluctuations of the determining intercomponent electronic coupling when occurring within closely coupled semi-rigid compact assemblies [114,166,167]. As highlighted above, the level of restriction of torsional motion about θ_1 impacts the intramolecular (here: intercomponent) electronic coupling, which is *smaller* within *constrained* **5-Os** dyad than within the only *restrained* **4-Os** dyad. As a matter of fact, the Dexter mechanism for electronic energy transfer (relying on orbital overlap and corresponding to a double electron transfer), which is most likely operative in the present case of closely coupled dyads (see Section 1.2.3), is very sensitive to electronic coupling (and definitively more than for ET). Hence, it can be foreseen that the EnT decay is slowed down to a much larger extent than the ET on passing from **4-Os** to **5-Os**. In other words, whereas reversible EnT (equilibration process) is still competitive in **4-Os**, this is no longer the case in the **5-Os** constrained dyad, which shows a weaker intercomponent electronic coupling because of its locked intramolecular geometrical decoupling.

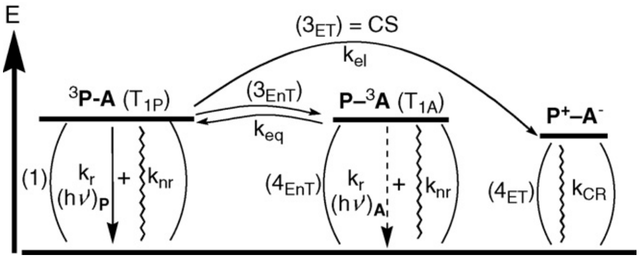

Fig. 11. Schematic energy diagram illustrating the photochemistry taking place within **4-Os** and **5-Os** (see ref. [115b] for details). In **4-Os**, energy equilibration (path 3_{EnT}; k_{eq}) competes with charge separation (CS, path 3_{ET}; k_{el}). In **5-Os**, reversible energy transfer (path 3_{EnT}) between **P** and **A** is no longer competitive with charge separation (path 3_{ET}). In both cases, deactivation from the T_{1A} triplet of excited acceptor (path 4_{EnT}) is much less efficient than decay from the T_{1P} of photoexcited **P** (path 1), which is itself much less efficient than charge recombination (CR) from the **P$^+$–A$^-$** charge-separated state (path 4_{ET}).

Given that **4-Os** and **5-Os** are both **P1-($\boldsymbol{\theta_1}$)-A** dyad supermolecules, changing the level of restraint for torsional motion attached to "spacing" twist angle θ_1 that is, the mean electronic coupling between **P1** and **A**, is here changing the balance between competing PET and PEnT intercomponent processes [168]. The emission properties are switched accordingly from virtually non-emissive for **P$_{\mathbf{tpy}}$1** within **5-Os** (due to dominating intramolecular oxidative quenching of ***P** and CSS formation) to increased emission lifetime for **4-Os** (due to intervening reversible electronic energy transfer that is, equilibration between the **P**-centered ^{3}MLCT state and an **A**-centered triplet LES). The overall phenomenon is referred to as the "conformational gating of photoinduced processes".

5. Conformational gating for molecular switching and sensing

The point is that conformationally related *large* and *supramolecular* species (Section 1.2.3) can show sharply different emission properties, as illustrated by case studies B and C (Sections 3 and 4), so that implementation of conformational gating for optical switching [45] or sensing [169] can be envisioned.

We distinguish between two cases relying on the conformational tuning of intramolecular electronic coupling: (i) the status of the overall molecular assembly is switched from that of a *large* molecule to that of a *supermolecule* (and vice versa) upon properly changing intramolecular conformation about the determining linkage of a bipartite assembly (case of **1-bpy**/**1-phen**) and (ii), the balance between two competing intramolecular photoinduced processes (namely PET and PEnT) within a closely coupled supramolecular species is changed by modifying intramolecular conformation (or the level of restriction of intramolecular torsional motion about a key linkage; case of **4-Os**/**5-Os**) and so the emission features of the luminophore accordingly.

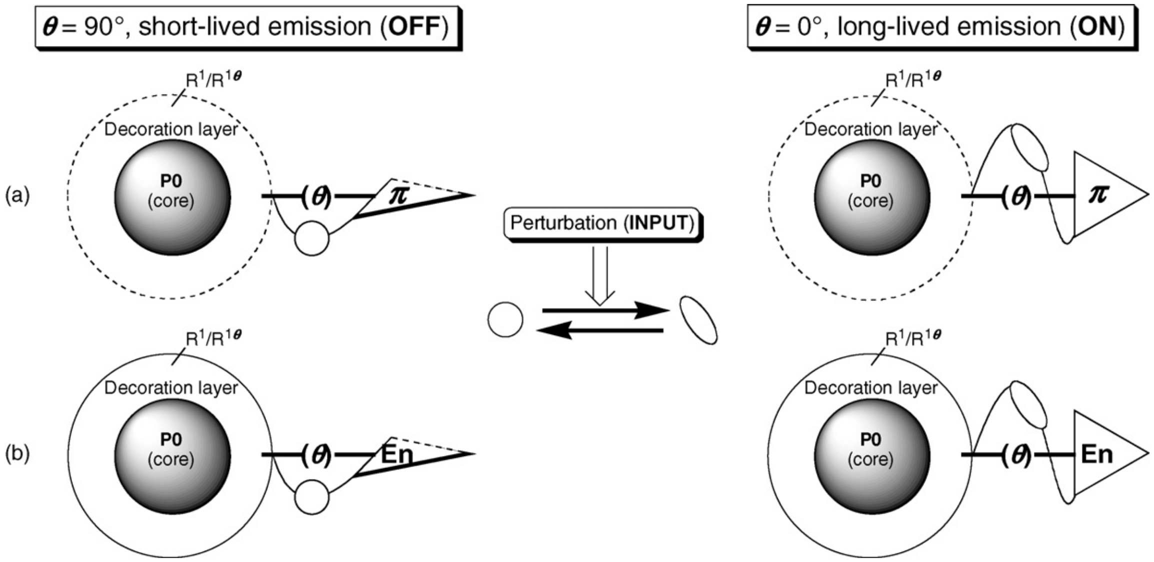

Fig. 12. Two possible implementations of the conformational gating for molecular sensing (or switching): (a) using a $R^{1\theta}$ substituent as a *potential* π-extending domain (top) or (b), using a remote site (**RS**) as a *potential* energy reservoir (bottom).

In principle, obtaining switchable light-emitting PMDs should be possible by harnessing properly, with a mechanically active linker (actuator), bipartite assemblies comprised of a luminophore and of a potentially interplaying remote site or π-extension. At one and the same time, the "smart linker" should interplay with an external stimulus (whether chemical, redox, photonic, or other) and undergo a structural change (e.g. elongation/contraction) upon interacting with this trigger [47]. The aim is to mechanically control the interaction between the two subunits by an external stimulus via a conformational modulation of intramolecular electronic coupling. In the present case, potential applications are essentially envisioned for molecular sensors no longer relying on a change of the emission *intensity* of the probe but rather on a change of its emission *lifetime*, instead [170].

Two main principles are of interest here, based on the monitoring of an intramolecular conformation: (i) to change the electronic accessibility of a π-extending domain appended to a poor luminophore (Fig. 12a) and (ii), to change the electronic availability of a remote energy reservoir (Fig. 12b). In both cases, the conformational gating of the intramolecular electronic coupling and attached photoinduced processes is aimed essentially at changing the emission lifetime of the luminophoric probe.

6. Conclusions

To summarize, the entity which absorbs light is not necessarily the same as the one which re-emits light, even if there is no intervening "chemical" change but only transient conformational change(s). In other word, the ground-state species absorbing light may be – sharply – different from the excited-state luminophoric species. These conformational changes can be photoinduced (resulting from intramolecular charge redistribution in the excited state) such as *planarization*, which eventually impacts the photophysical features of the luminophore. Vice versa, mechanically changing intramolecular conformation (e.g. the degree of a geometrical decoupling or the level of restriction of a torsional motion) can impact in its turn the electronic/photophysical/photochemical behavior of the photoactive molecules to a complete change of its electronic/photophysical status (supermolecule versus large molecule) via a modification of intramolecular electronic coupling. This interplay between structure (conformation) and photophysical properties can be turned to good account to design PMDs perfected for molecular sensing or switching. As a matter of fact, the switching behavior performed on a conformational basis is preferably achieved with compact, closely coupled, assemblies.

Acknowledgements

P.P.L. is indebted to the French ministry of research for funding (ACI project no. JC4123). S.C. also acknowledge MIUR (FIRB and PRIN projects) for funding. We thank Edmond Amouyal, Claudio Chiorboli, Ilaria Ciofini, Carlo Adamo, Fethi Bedioui, Valérie Marvaud, Fabien Tuyèras and Jérôme Fortage for their various contributions.

References

[1] Among complexes of transition metals of the *d*-block, the scope of the paper is restricted to non-porphyrinic systems.
[2] T.J. Meyer, Pure Appl. Chem. 58 (1986) 1193.
[3] G.A. Crosby, J. Chem. Ed. 60 (1983) 791.
[4] N.P. Ayala, C.M. Flynn Jr., L.A. Sacksteder, J.N. Demas, B.A. DeGraff, J. Am. Chem. Soc. 112 (1990) 3837.
[5] This is not actually the case for chemical reasons: polypyridyl ligands are not soft enough for Ir(III) and Rh(III) "soft" metals (C.M. Flynn Jr., J.N. Demas, J. Am. Chem. Soc. 96 (1974) 1959) and are worth replaced by cyclometalating anionic ligands.
[6] N.E. Leadbeater, Comments Inorg. Chem. 20 (1998) 57.
[7] A. Vlcek Jr., Coord. Chem. Rev. 200–202 (2000) 933.
[8] J.N. Demas, G.A. Crosby, J. Am. Chem. Soc. 92 (1970) 7262.
[9] M. Kasha, Faraday Soc. Discuss. 9 (1950) 14.
[10] A.W. Adamson, J. Chem. Ed. 60 (1983) 797.
[11] J.K. McCusker, Acc. Chem. Res. 36 (2003) 876.
[12] G. Malouf, P.C. Ford, J. Am. Chem. Soc. 99 (1977) 7213.
[13] (a) K. Szacilowski, W. Macyk, G. Stochel, Z. Stasicka, S. Sostero, O. Traverso, Coord. Chem. Rev. 208 (2000) 277;
(b) K. Szacilowski, Z. Stasicka, Coord. Chem. Rev. 229 (2002) 17.
[14] P. Coppens, I. Novozhilova, A. Kovalevsky, Chem. Rev. 102 (2002) 861.
[15] J.J. Rack, J.R. Winkler, H.B. Gray, J. Am. Chem. Soc. 123 (2001) 2432.
[16] (a) I. Ciofini, C.A. Daul, C. Adamo, J. Phys. Chem. A 107 (2003) 11182;
(b) I. Ciofini, P.P. Lainé, F. Bedioui, C.A. Daul, C. Adamo, C. R. Chimie 9 (2006) 226.
[17] D.R. McMillin, K.M. McNett, Chem. Rev. 98 (1998) 1201.
[18] D.V. Scaltrito, D.W. Thompson, J.A. O'Callaghan, G.J. Meyer, Coord. Chem. Rev. 208 (2000) 243.
[19] N. Armaroli, Chem. Soc. Rev. 30 (2001) 113.
[20] G.B. Shaw, C.D. Grant, H. Shirota, E.W. Castner Jr., G.J. Meyer, L.X. Chen, J. Am. Chem. Soc. 129 (2007) 2147.
[21] M. Iwamura, S. Takeuchi, T. Tahara, J. Am. Chem. Soc. 129 (2007) 5248.
[22] J.J. McGarvey, I. Lawthers, J. Chem. Soc. Chem. Commun. (1982) 906.

[23] (a) S. Descurtins, P. Gütlich, C.P. Köhler, H. Spiering, A. Hauser, Chem. Phys. Lett. 105 (1984) 1;
(b) S. Decurtins, P. Gütlich, K.M. Hasselbach, A. Hauser, H. Spiering, Inorg. Chem. 24 (1985) 2174;
(c) A. Hauser, Chem. Phys. Lett. 124 (1986) 543.

[24] N. Sutin, C. Creutz, J. Chem. Ed. 60 (1983) 809.

[25] V. Balzani, Tetrahedron 48 (1992) 10443.

[26] V. Balzani, F. Scandola, Supramolecular Photochemistry, Ellis Horwood, Chichester, UK, 1991 (Chapter 12).

[27] V. Balzani, L. Moggi, F. Scandola, in: V. Balzani (Ed.), Supramolecular Photochemistry, D. Reidel Publishing Co., Dordrecht, The Netherlands, 1987, p. 1.

[28] For a recent review in the field, refer to V. Balzani, G. Bergamini, S. Campagna, F. Puntoriero, Top. Curr. Chem. 280 (2007) 1.

[29] V. Balzani, A. Juris, Coord. Chem. Rev. 211 (2001) 97.

[30] T.J. Meyer, Pure Appl. Chem. 62 (1990) 1003.

[31] State-of-the-Art Symposium: Inorganic Photochemistry. Hoffman, M.Z. (ed.), J. Chem. Ed. 60 (1983) (special issue).

[32] Concepts in Inorganic Photochemistry, A.W. Adamson, P.D. Fleischauer (eds.), Wiley-Interscience, New-York, 1975.

[33] V. Balzani, V. Carassiti, Photochemistry of Coordination Compounds, Academic Press, London, 1970.

[34] J.-M. Lehn, Angew. Chem. Int. Ed. 29 (1990) 1304.

[35] T.J. Meyer, Acc. Chem. Res. 22 (1989) 163.

[36] V. Balzani, Photochem. Photobiol. Sci. 2 (2003) 459.

[37] W.R. Browne, N.M. O'Boyle, J.J. McGarvey, J.G. Vos, Chem. Soc. Rev. 34 (2005) 641.

[38] Th. Förster, Discuss. Faraday Soc. 27 (1959) 7.

[39] Flexibility of the linker sometimes makes intervening electron-exchange collisional interactions possible (hereafter referred to as Dexter mechanism).

[40] D.L. Dexter, J. Chem. Phys. 21 (1953) 836.

[41] (a) K. Ohkubo, H. Kotani, J. Shao, Z. Ou, K.M. Kadish, G. Li, R.K. Pandey, M. Fujitsuka, O. Ito, H. Imahori, S. Fukuzumi, Angew. Chem. Int. Ed. 43 (2004) 853;
(b) S. Fukuzumi, H. Kotani, K. Ohkubo, S. Ogo, N.V. Tkachenko, H. Lemmetyinen, J. Am. Chem. Soc. 126 (2004) 1600.

[42] A. Harriman, Angew. Chem. Int. Ed. 43 (2004) 4985.

[43] J.W. Verhoeven, H.J. van Ramesdonk, M.M. Groeneveld, A.C. Benniston, A. Harriman, Chem. Phys. Chem. 6 (2005) 2251.

[44] A. Harriman, L.J. Mallon, G. Ulrich, R. Ziessel, Chem. Phys. Chem. 8 (2007) 1207.

[45] P.P. Lainé, I. Ciofini, P. Ochsenbein, E. Amouyal, C. Adamo, F. Bedioui, Chem. Eur. J. 11 (2005) 3711.

[46] These effects are generally related to switching principles implemented for molecular actuators or motors.

[47] Selected recent references concerning molecular actuation;
(a) T. Ikeda, J.-I. Mamiya, Y. Yu, Angew. Chem. Int. Ed. 46 (2007) 506;
(b) M.F. Hawthorne, B.M. Ramachandran, R.D. Kennedy, C.B. Knobler, Pure Appl. Chem. 78 (2006) 1299;
(c) A. Almutairi, K. Yoon, F. Tham, M.J. Marsella, Pure Appl. Chem. 78 (2006) 777;
(d) J. Casanovas, D. Zanuy, C. Alemán, Angew. Chem. Int. Ed. 45 (2006) 1103;
(e) G.S. Kottas, L.I. Clarck, D. Horinek, J. Michl, Chem. Rev. 105 (2005) 1281;
(f) B. Jousselme, P. Blanchard, N. Gallego-Planas, J. Delaunay, M. Allain, P. Richomme, E. Levillain, J. Roncali, J. Am. Chem. Soc. 125 (2003) 2888;
(g) B. Jousselme, P. Blanchard, E. Levillain, J. Delaunay, M. Allain, P. Richomme, D. Rondeau, N. Gallego-Planas, J. Roncali, J. Am. Chem. Soc. 125 (2003) 1363;
(h) B.L. Feringa, Acc. Chem. Res. 31 (2001) 504;
(i) A. Robertson, S. Shinkai, Coord. Chem. Rev. 205 (2000) 157.

[48] Z.R. Grabowski, K. Rotkiewicz, W. Rettig, Chem. Rev. 103 (2003) 3899 (and references therein).

[49] (a) A. Almenningen, O. Bastiansen, L. Fernholt, B.N. Cyvin, S.J. Cyvin, S. Samdal, J. Mol. Struct. 128 (1985) 59;
(b) K. Furuya, H. Torii, Y. Furukawa, M. Tasumi, Theochem 424 (1998) 225.

[50] (a) K. Honda, Y. Furukawa, K. Furuya, H. Torii, M. Tasumi, J. Phys. Chem. A 106 (2002) 3587;
(b) J.L. Brédas, B. Thémans, J.G. Fripiat, J.M. André, R.R. Chance, Phys. Rev. B 29 (1984) 6761.

[51] M. Malagoli, J.L. Bredas, Chem. Phys. Lett. 327 (2000) 13.

[52] E. Zojer, J. Cornil, G. Leising, J.L. Brédas, Phys. Rev. B 59 (1999) 7957.

[53] (a) W.J.D. Beenken, H. Lischka, J. Chem. Phys. 123 (2005) 144311;
(b) I. Vragovic, E.M. Calzado, M.A. Diaz Garcia, Chem. Phys. 332 (2007) 48.

[54] A. Juris, V. Balzani, F. Barigelletti, S. Campagna, P. Belser, A. Von Zelewsky, Coord. Chem. Rev. 84 (1988) 85.

[55] The term *planarization* specifically refers to the molecular *structural relaxation* towards planarity occurring on going from the ground state to the lowest thexi state.

[56] The role of the solvent (especially polarity), which can be determining in some peculiar cases such as for TICT effect [48], is not discussed in the present review. To overcome possible biases related to solvent contributions, comparative studies herein reported (Sections 2, 3 and 4) were carried out under the same experimental conditions including the nature of the surrounding medium (nitrile solvents) and temperature. For solvent dependence of large structural rearrangements, see:
(a) D.J. Liard, C.J. Kleverlaan, A. Vlcek Jr., Inorg. Chem. 42 (2003) 7995;
(b) P.F. Barbara, T.J. Meyer, M.A. Ratner, J. Phys. Chem. 100 (1996) 13148.

[57] Luminescence is however a means of choice to probe intramolecular medium and photoinduced events occurring at this level.

[58] C. Kutal, J. Chem. Ed. 60 (1983) 882.

[59] J.R. Bolton, Science 202 (1978) 705.

[60] V. Balzani, L. Moggi, M.F. Manfrin, F. Bolletta, M. Gleria, Science 189 (1975) 852.

[61] E. Amouyal, Solar Energy Mater. Solar Cells 38 (1995) 249.

[62] A. Juris, F. Barigelletti, V. Balzani, P. Belser, A. von Zelewsky, Israel J. Chem. 22 (1982) 87.

[63] In the real world, this lower limit is actually never reached due to non-unity quantum yields of photochemical processes together with unavoidable losses of energy attached to various intervening energy conversion steps; see for instance [58–60]. A more realistic threshold energy for water splitting could probably be located at about 1.60 eV.

[64] D.G. Whitten, Acc. Chem. Res. 13 (1980) 83.

[65] UV-absorption attached to the presence of organic ligands is useful as collected energy cascades to the lowest thexi state by virtue of the Crosby rules.

[66] V. Balzani, A. Juris, M. Venturi, S. Campagna, S. Serroni, Chem. Rev. 96 (1996) 759.

[67] For a recent review in the field, refer to;
M.T. Indelli, C. Chiorboli, F. Scandola, Top. Curr. Chem. 280 (2007) 215.

[68] For a recent review in the field, refer to;
L. Flamigni, A. Barbieri, C. Sabatini, B. Ventura, F. Barigelletti, Top. Curr. Chem. 281 (2007) 143.

[69] For a recent review in the field, refer to;
R.A. Kirgan, B.P. Sullivan, D.P. Rillema, Top. Curr. Chem. 281 (2007) 45.

[70] For a recent review in the field, refer to;
S. Campagna, F. Puntoriero, F. Nastasi, G. Bergamini, V. Balzani, Top. Curr. Chem. 280 (2007) 117.

[71] For a recent review in the field, refer to;
D. Kumaresan, K. Shankar, S. Vaidya, R.H. Schmehl, Top. Curr. Chem. 281 (2007) 101.

[72] $h\nu_1$ in Figure 3.

[73] $h\nu_2$ in Figure 3.

[74] J.N. Demas, D.G. Taylor, Inorg. Chem. 18 (1979) 3177.

[75] W.E. Ford, M.A.J. Rodgers, J. Phys. Chem. 96 (1992) 2917.

[76] When the complex photosensitizer undergoes an equilibration process with a remote chromophore within a $\mathbf{P}\sim\mathbf{RS}$ assembly, its behavior (function) oscillates between that of an energy-donor ($^{*}\mathbf{P} = \mathbf{D}$ while $\mathbf{RS} = \mathbf{A}$) and that of an energy-acceptor ($\mathbf{P} = \mathbf{A}$ while $^{*}\mathbf{RS} = \mathbf{D}$) as a function of time.

[77] N.D. McClenaghan, Y. Leydet, B. Maubert, M.T. Indelli, S. Campagna, Coord. Chem. Rev. 249 (2005) 1336.

[78] Note while it can increase the lifetime of emission, this approach cannot increase emission quantum yields or yields of any intercomponent process; see ref. [77]. Moreover, a long-lived thexi state is not a necessary requisite for functioning molecular devices or light-energy conversion. Thus, in the case of Grätzel photovoltaic cells, ultrafast electron injection into semiconductors can occur from "hot" (i.e. non-relaxed) or short-lived MLCT states; see for instance;
Y. Tachibana, J.E. Moser, M. Grätzel, D.R. Klug, J.R. Durrant, J. Phys. Chem. 100 (1996) 20056.

[79] X.-Y. Wang, A. Del Guerzo, R.H. Schmehl, J. Photochem. Photobiol. C 5 (2004) 55.

[80] E.C. Constable, Chem. Soc. Rev. 36 (2007) 246.

[81] L. Spiccia, G.B. Deacon, C.M. Kepert, Coord. Chem. Rev. 248 (2004) 1329.

[82] A comprehensive overview of the "quest for long-lived excited-states at room temperature for Ru(II) complexes of tridentate ligands" is provided by;
E.A. Medlycott, G.S. Hanan, Coord. Chem. Rev. 250 (2006) 1763.

[83] P.A. Anderson, F.R. Keene, T.J. Meyer, J.A. Moss, G.F. Strouse, J.A. Treadway, J. Chem. Soc. Dalton Trans. (2002) 3820.

[84] M. Maestri, N. Armaroli, V. Balzani, E.C. Constable, A.M.W. Cargill Thompson, Inorg. Chem. 34 (1995) 2759.

[85] P.A. Anderson, G.B. Deacon, K.H. Haarmann, F.R. Keene, T.J. Meyer, D.A. Reitsma, B.W. Skelton, G.F. Strouse, N.C. Thomas, J.A. Treadway, A.H. White, Inorg. Chem. 34 (1995) 6145.

[86] J.-P. Sauvage, J.-P. Collin, J.-C. Chambron, S. Guillerez, C. Coudret, V. Balzani, F. Barigelleti, L. De Cola, L. Flamigni, Chem. Rev. 94 (1994) 993.

[87] J.A. Treadway, B. Loeb, R. Lopez, P.A. Anderson, F.R. Keene, T.J. Meyer, Inorg. Chem. 35 (1996) 2242.

[88] E.M. Kober, J.L. Marshall, W.J. Dressick, B.P. Sullivan, J.V. Caspar, T.J. Meyer, Inorg. Chem. 24 (1985) 2755.

[89] (a) M.J. Cook, A.P. Lewis, G.S.G. McAuliffe, V. Skarda, A.J. Thomson, J.L. Glasper, D.J. Robbins, J. Chem. Soc. Perkin Trans. II (1984) 1293;
(b) M.J. Cook, A.P. Lewis, G.S.G. McAuliffe, V. Skarda, A.J. Thomson, J.L. Glasper, D.J. Robbins, J. Chem. Soc. Perkin Trans. II (1984) 1303.

[90] E.C. Constable, A.M.W. Cargill Thompson, D.A. Tocher, M.A.M. Daniels, New. J. Chem. 16 (1992) 855.

[91] H.-F. Suen, S.W. Wilson, M. Pomerantz, J.L. Walsh, Inorg. Chem. 28 (1989) 786.

[92] H.B. Ross, M. Boldaji, D.P. Rillema, C.B. Blanton, R.P. White, Inorg. Chem. 28 (1989) 1013.

[93] B. Durham, J.L. Walsh, C.L. Carter, T.J. Meyer, Inorg. Chem. 19 (1980) 860 (and references cited therein).

[94] (a) J. Van Houten, R.J. Watts, J. Am. Chem. Soc. 98 (1976) 4853;
(b) J. Van Houten, R.J. Watts, Inorg. Chem. 17 (1978) 3381.

[95] First demonstrated for $[\mathrm{Ru(bpy)_3}]^{2+}$ in water (see ref. [94]), photolabilization can be overcome by reinforcing the chelate effect (using caging oligopyridyl ligands; see: F. Barigelletti, L. De Cola, V. Balzani, P. Belser, A. von Zelewsky, F. Vögtle, F. Ebmeyer, S. Grammenudi, J. Am. Chem. Soc. 111 (1989) 4662.) and by choosing non-coordinating counter-anions such as hexafluorophosphate ($\mathrm{PF_6}^-$).

[96] E.C. Constable, G. Baum, E. Bill, R. Dyson, R. Van Eldik, D. Fenske, S. Kaderli, D. Morris, A. Neubrand, M. Neuburger, D.R. Smith, K. Wieghardt, M. Zehnder, A.D. Zuberbühler, Chem. Eur. J. 5 (1999) 498.

[97] P. Mobian, J.-M. Kern, J.-P. Sauvage, Angew. Chem. Int. Ed. 43 (2004) 2392.

[98] Overall axial geometry is indeed highly desirable for PMDs meant to perform vectorial PEnT and PET (CS state formation) for artificial photosynthesis purposes, and is therefore one of the salient prerequisites for the **P** component, see ref. [86].

[99] (a) M. Jäger, L. Eriksson, J. Bergquist, O. Johansson, J. Org. Chem. 72 (2007) 10227;
(b) M. Abrahamsson, H.-C. Becker, L. Hammarström, C. Bonnefous, C. Chamchoumis, R.P. Thummel, Inorg. Chem. 46 (2007) 10354;
(c) M. Abrahamsson, M. Jäger, T. Österman, L. Eriksson, P. Persson, H.-C. Becker, O. Johansson, L. Hammarström, J. Am. Chem. Soc. 128 (2006) 12616;
(d) M. Abrahamsson, H. Wolpher, O. Johansson, J. Larsson, M. Kritikos, L. Eriksson, P.-O. Norrby, J. Bergquist, L. Sun, B. Åkermark, L. Hammarström, Inorg. Chem. 44 (2005) 3215;
(e) H. Wolpher, O. Johansson, M. Abrahamsson, M. Kritikos, L. Sun, B. Åkermark, Inorg. Chem. Commun. 7 (2004) 337.

[100] G.F. Strouse, J.R. Schoonover, R. Duesing, S. Boyde, W.E. Jones Jr., T.J. Meyer, Inorg. Chem. 34 (1995) 473.

[101] C. Goze, J.-C. Chambron, V. Heitz, D. Pomeranc, X.J. Salom-Roig, J.-P. Sauvage, A. Farran Morales, F. Barigelletti, Eur. J. Inorg. Chem. (20) (2003) 3752.

[102] With respect to $-M$ substituents, the correlation between the modification of π extension within the ligand and the strength of the ligand field can be illustrated by the ligand-driven light-induced spin change (LD-LISC) effect. Indeed, subsequent to cis-to-trans photo-isomerization of the styryl decoration ($-M$) of styryl-pyridine ligands of a properly designed high-spin iron(II) complex, a metal-centered spin-crossover phenomenon (from high-spin to low-spin) occurs. Such an effect can be straightforwardly ascribed to the strengthening of the ligand field, which is accompanied by a greater splitting of d orbital (Δ), therefore directly related to the lowering of the energy of the π^* orbital (LUMO) when intra-ligand conjugation becomes greater, see;
C. Roux, J. Zarembowitch, B. Gallois, T. Granier, R. Claude, Inorg. Chem. 33 (1994) 2273.

[103] J.V. Caspar, E.M. Kober, B.P. Sullivan, T.J. Meyer, J. Am. Chem. Soc. 104 (1982) 630.

[104] L. Hammarström, F. Barigelletti, L. Flamigni, M.T. Indelli, N. Armaroli, G. Calogero, M. Guardigli, A. Sour, J.-P. Collin, J.-P. Sauvage, J. Phys. Chem. A 101 (1997) 9061.

[105] J.A. Treadway, G.F. Strouse, R.R. Ruminski, T.J. Meyer, Inorg. Chem. 40 (2001) 4508.

[106] S.M. Draper, D.J. Gregg, E.R. Schofield, W.R. Browne, M. Duati, J.G. Vos, P. Passaniti, J. Am. Chem. Soc. 126 (2004) 8694.

[107] P.A. Anderson, G.F. Strouse, J.A. Treadway, F.R. Keene, T.J. Meyer, Inorg. Chem. 33 (1994) 3863.

[108] Y.-Q. Fang, N.J. Taylor, F. Laverdière, G.S. Hanan, F. Loiseau, F. Nastasi, S. Campagna, H. Nierengarten, E. Leize-Wagner, A. Van Dorsselaer, Inorg. Chem. 46 (2007) 2854.

[109] E.A. Medlycott, G.S. Hanan, Chem. Soc. Rev. 34 (2005) 133.

[110] J. Wang, Y.-Q. Fang, L. Bourget-Merle, M.I.J. Polson, G.S. Hanan, A. Juris, F. Loiseau, S. Campagna, Chem. Eur. J. 12 (2006) 8539.

[111] P. Lainé, F. Bedioui, P. Ochsenbein, V. Marvaud, M. Bonin, E. Amouyal, J. Am. Chem. Soc. 124 (2002) 1364.

[112] (a) Y.-Z. Hu, S. Tsukiji, S. Shinkai, S. Oishi, I. Hamachi, J. Am. Chem. Soc. 122 (2000) 241;
(b) Y.-Z. Hu, H. Takashima, S. Tsukiji, S. Shinkai, T. Nagamune, S. Oishi, I. Hamachi, Chem. Eur. J. 6 (2000) 1907.

[113] (a) T. Klumpp, M. Linsenmann, S.L. Larson, B.R. Limoges, D. Bürssner, E.B. Krissinel, C.M. Elliott, U.E. Steiner, J. Am. Chem. Soc. 121 (1999) 1076;
(b) E. Danielson, C.M. Elliott, J.W. Merkert, T.J. Meyer, J. Am. Chem. Soc. 109 (1987) 2519.

[114] I. Ciofini, P.P. Lainé, F. Bedioui, C. Adamo, J. Am. Chem. Soc. 126 (2004) 10763.

[115] (a) P.P. Lainé, F. Bedioui, F. Loiseau, C. Chiorboli, S. Campagna, J. Am. Chem. Soc. 128 (2006) 7510;
(b) P.P. Lainé, F. Loiseau, S. Campagna, I. Ciofini, C. Adamo, Inorg. Chem. 45 (2006) 5538;
(c) P. Lainé, F. Bedioui, E. Amouyal, V. Albin, F. Berruyer–Penaud, Chem. Eur. J. 8 (2002) 3162;
(d) P. Lainé, E. Amouyal, Chem. Commun. (1999) 935.

[116] M.R. Wasielewski, J. Org. Chem. 71 (2006) 5051.

[117] A.C. Benniston, A. Harriman, P. Li, P.V. Patel, C.A. Sams, J. Org. Chem. 71 (2006) 3481.

[118] G.J. Wilson, A. Launikonis, W.H.F. Sasse, A.W.-H. Mau, J. Phys. Chem. A 101 (1997) 4860.

[119] A. Harriman, M. Hissler, A. Khatyr, R. Ziessel, Chem. Commun. (1999) 735.

[120] A.C. Benniston, G. Chapman, A. Harriman, M. Mehrabi, C.A. Sams, Inorg. Chem. 43 (2004) 4227.

[121] J.A. Simon, S.L. Curry, R.H. Schmehl, T.R. Schatz, P. Piotrowiak, X. Jin, R.P. Thummel, J. Am. Chem. Soc. 119 (1997) 11012.

[122] In this case, **P** behaves as an energy acceptor with respect to photo-excited **RS** (***A**), which acts as an energy donor. Such a type of energy transfer from peripheral chromophoric units (***RS**) to a "central" energy-collecting emitter (**P**) is encountered in the case of PMDs functioning as antenna systems (light-harvesting purposes) [27].

[123] From the viewpoint of emission of **P**, the decay of T_1 is twofold: comprising a fast component attached to regular population of T_1 from S_1, and a slow component attached to the delayed population of T_1.

[124] I. Ciofini, P.P. Lainé, M. Zamboni, C.A. Daul, V. Marvaud, C. Adamo, Chem. Eur. J. 13 (2007) 5360.

[125] (a) R. Passalacqua, F. Loiseau, S. Campagna, Y.-Q. Fang, G.S. Hanan, Angew. Chem. Int. Ed. 42 (2003) 1608;
(b) Y.-Q. Fang, N.J. Taylor, G.S. Hanan, F. Loiseau, R. Passalacqua, S. Campagna, H. Nierengarten, A. Van Dorsselaer, J. Am. Chem. Soc. 124 (2002) 7912.

[126] The electron-withdrawing and π-extending effects of the prmd substituent contribute to the lowering of the energy of T_1, thus allowing it to match with the energy of the T_{1A} of anthracene (T_1 and T_{1A} are roughly isoenergetic). When there is no such intervening prmd decoration (that is, direct appending of An to $[\mathrm{(tpy)Ru(tpy)}]^{2+}$), the lowest thexi state of $\mathbf{P0_{tpy}/Ru}$ lies at a significantly higher energy than the triplet of anthracene (T_{1A}), which therefore behaves as a quencher for T_1 (further deteriorating the already very poor luminescence properties of $\mathbf{P0_{tpy}/Ru}$!), see;
G. Albano, V. Balzani, E.C. Constable, M. Maestri, D.R. Smith, Inorg. Chim. Acta 277 (1998) 225.

[127] C.R. Hecker, A.K.I. Gushurst, D.R. McMillin, Inorg. Chem. 30 (1991) 538.

[128] M.L. Stone, G.A. Crosby, Chem. Phys. Lett. 79 (1981) 169.

[129] M. Montalti, A. Credi, L. Prodi, M.T. Gandolfi, Handbook of Photochemistry, third ed., CRC Press, Taylor and Francis, 2006.

[130] (a) R.J. Watts, G.A. Crosby, J. Am. Chem. Soc. 94 (1972) 2606;
(b) R.J. Watts, G.A. Crosby, J. Am. Chem. Soc. 93 (1971) 3184.

[131] A. Ceulemans, L.G. Vanquickenborne, J. Am. Chem. Soc. 103 (1981) 2238.

[132] C.C. Phifer, D.R. McMillin, Inorg. Chem. 25 (1986) 1329.

[133] B.S. Brunschwig, C. Creutz, N. Sutin, Coord. Chem. Rev. 177 (1998) 61.

[134] J.-P. Collin, S. Guillerez, J.-P. Sauvage, F. Barigelletti, L. De Cola, L. Flamigni, V. Balzani, Inorg. Chem. 30 (1991) 4230.

[135] E. Amouyal, M. Mouallem-Bahout, G. Calzaferri, J. Phys. Chem. 95 (1991) 7641.

[136] N.H. Damrauer, T.R. Boussie, M. Devenney, J.K. McCusker, J. Am. Chem. Soc. 119 (1997) 8253.

[137] N.H. Damrauer, B.T. Weldon, J.K. McCusker, J. Phys. Chem. A 102 (1998) 3382.

[138] N.H. Damrauer, J.K. McCusker, J. Phys. A Chem. 103 (1999) 8440.

[139] For instance, in the case of hexa-phenylated $\mathbf{P0_{bpy}/Ru}$ core, decorated at 4 and 4′ positions, the emission quantum yield (Φ_{em}) increases four-fold on passing from native $\mathbf{P0_{bpy}/Ru}$ ($\Phi_{em} = 0.123$) to $\mathbf{P_{bpy}1^{ph2}/Ru}$ ($\Phi_{em} = 0.480$) in deaerated CH_2Cl_2, see;
W.E. Jones Jr., R.A. Smith, M.T. Abramo, M.D. Williams, J. Van Houten, Inorg. Chem. 28 (1989) 2281.

[140] K.F. Freed, J. Jortner, J. Chem. Phys. 52 (1970) 6272.

[141] Actually, on realizing the nature of the gap between experimental observations and original expectations [109], Hanan and Campagna proposed to replace phenyl decoration with the 2-pyrimidinyl extension so as to minimize interannular steric hindrance about θ_0 and fully take advantage of beneficial effects of intraligand electron delocalization [125b] (cf. Section 1.4.4.1).

[142] C. Berg-Brennan, P. Subramanian, M. Absi, C. Stern, J.T. Hupp, Inorg. Chem. 35 (1996) 3719.

[143] Even though methyl substituents do have a weak (inductive) electron-donating effect actually reflected by photophysical data, *Me₂bpy* and *ttpy* ligands are respectively denoted as *bpy* and *ptpy* for the sake of clarifying the discussion (nomenclature abbreviation).

[144] (a) M. Busby, D.J. Liard, M. Motevalli, H. Toms, A. Vlcek Jr., Inorg. Chim. Acta 357 (2004) 167;
(b) D.J. Liard, M. Busby, I.R. Farrell, P. Matousek, M. Towrie, A. Vlcek Jr., J. Phys. Chem. A 108 (2004) 556.

[145] Y. Shen, K.A. Walters, K. Abboud, K.S. Schanze, Inorg. Chim. Acta 300–302 (2000) 414.

[146] P. Chen, M. Curry, T.J. Meyer, Inorg. Chem. 28 (1989) 2271.

[147] M. Valásek, J. Pecka, J. Jindrich, G. Calleja, P.R. Craig, J. Michl, J. Org. Chem. 70 (2005) 405.

[148] For instance, when there are methyl groups on either sides of the (carbon) atom linked to the bpy ring instead of phenyl groups ortho to the $N_{\mathrm{pyridinio}}$ atom that is, within homoleptic ruthenium complex with 4,4′-dimesityl-substituted bpy ligands $\mathbf{P_{bpy}1^{Mes2}/Ru}$, averaging over the six dihedral angles θ_0 of the complex affords a value of ca. $70 \pm 10^\circ$ (crystallographic data) [136].

[149] C.R. Bock, J.A. Connor, A.R. Gutierrez, T.J. Meyer, D.G. Whitten, B.P. Sullivan, J.K. Nagle, J. Am. Chem. Soc. 101 (1979) 4815.

[150] (a) J.V. Caspar, T.J. Meyer, Inorg. Chem. 22 (1983) 2444;
(b) J.V. Caspar, T.J. Meyer, J. Am. Chem. Soc. 105 (1983) 5583.

[151] J.M. Calvert, J.V. Caspar, R.A. Binstead, T.D. Westmoreland, T.J. Meyer, J. Am. Chem. Soc. 104 (1982) 6620.

[152] P.D. Beer, Z. Chen, A. Grieve, J. Haggitt, J. Chem. Soc. Chem. Commun. (1994) 2413.

[153] A.C. Benniston, A. Harriman, Chem. Soc. Rev. 35 (2006) 169.

[154] (a) A.C. Benniston, A. Harriman, P. Li, P.V. Patel, J.P. Rostron, C.A. Sams, J. Phys. Chem. A 110 (2006) 9880;

(b) A.C. Benniston, A. Harriman, P. Li, P.V. Patel, C.A. Sams, Phys. Chem. Chem. Phys. 7 (2005) 3677;
(c) A.C. Benniston, A. Harriman, P. Li, C.A. Sams, M.D. Ward, J. Am. Chem. Soc. 126 (2004) 13630;
(d) A.C. Benniston, A. Harriman, P. Li, C.A. Sams, Phys. Chem. Chem. Phys. 6 (2004) 875;
(e) A.C. Benniston, A. Harriman, P. Li, C.A. Sams, Tetrahedron Lett. 44 (2003) 4167.

[155] O. Johansson, M. Borgström, R. Lomoth, M. Palmblad, J. Bergquist, L. Hammarström, L. Sun, B. Åkermark, Inorg. Chem. 42 (2003) 2908.

[156] S.E. Miller, A.S. Lukas, E. Marsh, P. Bushard, M.R. Wasielewski, J. Am. Chem. Soc. 122 (2000) 7802 (and references therein).

[157] (a) M.D. Ward, Chem. Soc. Rev. 24 (1995) 121;
(b) D.T. Pierce, W.E. Geiger, Inorg. Chem. 33 (1994) 373;
(c) T.-Y. Dong, C.-H. Huang, C.-K. Chang, Y.-S. Wen, S.-L. Lee, J.-A. Chen, W.-Y. Yeh, A. Yeh, J. Am. Chem. Soc. 115 (1993) 6357;
(d) S. Larson, J. Am. Chem. Soc. 103 (1981) 4034;
(e) M. Tanner, A. Ludi, Inorg. Chem. 20 (1981) 2348;
(f) H. Fisher, G.M. Tom, H. Taube, J. Am. Chem. Soc. 98 (1976) 5512.

[158] G. Tapolsky, R. Duesing, T.J. Meyer, Inorg. Chem. 28 (1990) 2285.

[159] (a) A. Gourdon, New. J. Chem. 16 (1992) 953;
(b) S. Woitellier, J.-P. Launay, C. Joachim, Chem. Phys. 131 (1989) 481.

[160] A.J. Amoroso, A. Das, J.A. McCleverty, M.D. Ward, F. Barigelletti, L. Flamigni, Inorg. Chim. Acta 226 (1994) 171.

[161] G.L. Gaines III, M.P. O'Neil, W.A. Svec, M.P. Niemczyk, M.R. Wasielewski, J. Am. Chem. Soc. 113 (1991) 719.

[162] N.I. Nijegorodov, W.S. Downey, J. Phys. Chem. 98 (1994) 5639 (and references therein).

[163] The decays reported are the best fit values derived from an analysis of the transient spectra decays performed at 20 probe wavelengths between 500 nm and 760 nm; see ref [115a].

[164] Intervening ultrafast planarization partly explains an intriguing subsequent non-linear optical response (including reverse saturable absorption) recorded for $\mathbf{P_{tpy}1^{ph}/M}$ (M = Ru, Os) photosensitizers and derived assemblies, see;
M. Konstantaki, E. Koudoumas, S. Couris, P. Lainé, E. Amouyal, S. Leach, J. Phys. Chem. B 105 (2001) 10797.

[165] A. Gabrielsson, P. Matousek, M. Towrie, F. Hartl, S. Zalis, A. Vlcek Jr., J. Phys. Chem. A 109 (2005) 6147.

[166] M. Cotlet, S. Masuo, G. Luo, J. Hofkens, M. Van der Auweraer, J. Verhoeven, K. Müllen, X.S. Xie, F. De Schryver, Proc. Natl. Acad. Sci. USA 101 (2004) 14343.

[167] E.A. Weiss, M.J. Tauber, R.F. Kelley, M.J. Ahrens, M.A. Ratner, M.R. Wasielewski, J. Am. Chem. Soc. 127 (2005) 11842.

[168] For other examples of interplay between the level of restriction of intramolecular conformation, intercomponent electronic coupling and occurrence of ET/EnT processes, see refs. [45,153,154,156,158] and also;
(a) S. Welter, N. Salluce, A. Benetti, N. Rot, P. Belser, P. Sonar, A.C. Grimsdale, K. Müllen, M. Lutz, A.L. Spek, L. De Cola, Inorg. Chem. 44 (2005) 4706 (and references therein);
(b) B. Schlicke, P. Belser, L. De Cola, E. Sabbioni, V. Balzani, J. Am. Chem. Soc. 121 (1999) 4207;
(c) F. Scandola, C. Chiorboli, M.T. Indelli, M.A. Rampi, in: V. Balzani (Ed.), Electron Transfer in Chemistry, vol. 3, Wiley-VCH, Weinheim, 2001, p. 337.

[169] C. McDonagh, C.S. Burke, B.D. MacCraith, Chem. Rev. 108 (2008) 400.

[170] B. Higgins, B.A. DeGraff, J.N. Demas, Inorg. Chem. 44 (2005) 6662.